



HAL
open science

Ostreopsis lenticularis Y. Fukuyo (Dinophyceae, Gonyaulacales) from French Polynesia (South Pacific Ocean)

Nicolas Chomérat, Gwenael Bilien, Amélie Derrien, Kévin Henry, André Ung, Jérôme Viallon, Hélène Taiana Darius, Clémence Mahana Iti Gatti, Mélanie Roué, Fabienne Hervé, et al.

► **To cite this version:**

Nicolas Chomérat, Gwenael Bilien, Amélie Derrien, Kévin Henry, André Ung, et al.. *Ostreopsis lenticularis* Y. Fukuyo (Dinophyceae, Gonyaulacales) from French Polynesia (South Pacific Ocean). *Harmful Algae*, 2019, 84, pp.95-111. 10.1016/j.hal.2019.02.004 . hal-03187307

HAL Id: hal-03187307

<https://hal.science/hal-03187307v1>

Submitted on 22 Oct 2021

HAL is a multi-disciplinary open access archive for the deposit and dissemination of scientific research documents, whether they are published or not. The documents may come from teaching and research institutions in France or abroad, or from public or private research centers.

L'archive ouverte pluridisciplinaire **HAL**, est destinée au dépôt et à la diffusion de documents scientifiques de niveau recherche, publiés ou non, émanant des établissements d'enseignement et de recherche français ou étrangers, des laboratoires publics ou privés.



Distributed under a Creative Commons Attribution - NonCommercial 4.0 International License

**1 *Ostreopsis lenticularis* Y. Fukuyo (Dinophyceae, Gonyaulacales) from French Polynesia (South
2 Pacific Ocean): a revisit of its morphology, molecular phylogeny and toxicity.**

3

4 Nicolas Chomérat^{1*}, Gwenael Bilien¹, Amélie Derrien¹, Kévin Henry², André Ung², Jérôme
5 Viallon², Hélène Taiana Darius², Clémence Mahana iti Gatti², Mélanie Roué³, Fabienne Hervé⁴,
6 Damien Réveillon⁴, Zouher Amzil⁴ and Mireille Chinain²

7

8 ¹IFREMER, LER BO, Station of Marine Biology of Concarneau, Place de la Croix, F-29900
9 Concarneau, France

10 ²Institut Louis Malardé, Laboratoire des Micro-algues toxiques, UMR 241-EIO, PO box 30, 98713
11 Papeete, Tahiti, French Polynesia

12 ³Institut de Recherche pour le Développement (IRD), UMR 241-EIO, PO box 529, 98713 Papeete,
13 Tahiti, French Polynesia

14 ⁴IFREMER, Phycotoxins Laboratory, BP 21105, F-44311 Nantes Cedex 3, France

15

16 *Corresponding author: nicolas.chomerat@ifremer.fr

17 Abstract

18 To date, the genus *Ostreopsis* comprises eleven described species, of which seven are toxigenic and
19 produce various compounds presenting a major threat to human and environmental health. The
20 taxonomy of several of these species however remains controversial, as it was based mostly on
21 morphological descriptions leading, in some cases, to ambiguous interpretations and even possible
22 misidentifications. The species *Ostreopsis lenticularis* was first described by Y. Fukuyo from
23 French Polynesia using light microscopy observations, but without genetic information associated.
24 The present study aims at revisiting the morphology, molecular phylogeny and toxicity of *O.*
25 *lenticularis* based on the analysis of 47 strains isolated from 4 distinct locales of French Polynesia,
26 namely the Society, Australes, Marquesas and Gambier archipelagos. Observations in light,
27 epifluorescence and field emission scanning electron microscopy of several of these strains
28 analyzed revealed morphological features in perfect agreement with the original description of *O.*
29 *lenticularis*. Cells were oval, not undulated, 60.5–94.4 µm in dorso-ventral length, 56.1–78.2 µm in
30 width, and possessed a typical plate pattern with thecal plates showing two sizes of pores.
31 Phylogenetic analyses inferred from the LSU rDNA and ITS–5.8S sequences revealed that the 47
32 strains correspond to a single genotype, clustering with a strong support with sequences previously
33 ascribed to *Ostreopsis* sp. 5. Clonal cultures of *O. lenticularis* were also established and further
34 tested for their toxicity using the neuroblastoma cell-based assay and LC-MS/MS analyses. None of
35 the 19 strains tested showed toxic activity on neuroblastoma cells, while LC-MS/MS analyses
36 performed on the strains from Tahiti Island (i.e. type locality) confirmed that palytoxin and related
37 structural analogs were below the detection limit. These findings allow to clarify unambiguously the
38 genetic identity of *O. lenticularis* while confirming previous results from the Western Pacific which
39 indicate that this species shows no toxicity, thus stressing the need to reconsider its current
40 classification within the group of toxic species.

42 Keywords

43 ITS-5.8S rDNA; LSU rDNA; microscopy; *Ostreopsis lenticularis*; taxonomy; toxins

44 1. Introduction

45 First described from the Gulf of Thailand in 1901 (Schmidt, 1901), the genus *Ostreopsis* Johs.
46 Schmidt has become a well-studied dinoflagellate due to its recurrent toxic blooms in several places
47 around the world and their deleterious impacts on both marine ecosystem functioning and human
48 health (Penna et al., 2010; Parsons et al., 2012; Accoroni and Totti, 2016; Verma et al., 2016).
49 Originally limited to tropical locales, this genus is now found in temperate areas where they cause
50 severe health problems (e.g. Tichadou et al., 2010; del Favero et al., 2012; Accoroni and Totti,
51 2016; Berdalet et al., 2017). *Ostreopsis* species have been shown to produce a variety of toxic
52 compounds (Lassus et al., 2016), that can bio-accumulate in marine organisms such as molluscs,
53 herbivorous echinoderms or fishes (Amzil et al., 2012; Brissard et al., 2014). The toxins produced
54 by *Ostreopsis* species are analogs of palytoxin (PITX), a toxin primarily isolated from the zoanthid
55 *Palythoa toxica* (Moore and Scheuer, 1971). So far, several toxin classes which share both similar
56 structure and site of action with PITX have been described, such as ostreocins -B and -D (OSTs)
57 (Usami et al., 1995; Ukena et al., 2001; Terajima et al., 2018), mascarenotoxins-a, b and c (McTXs)
58 (Lenoir et al., 2004; Rossi et al., 2010), and ovatoxins (OvTxS) (Ciminiello et al., 2008, 2010;
59 Sanchez et al., 2011; Ciminiello et al., 2012; Suzuki et al., 2012; Uchida et al., 2013; Brissard et al.,
60 2015; García-AltareS et al., 2015; Accoroni et al., 2016; Tartaglione et al., 2016, 2017). Other
61 compounds called ostreotoxins (OTXs) were reported but not yet structurally elucidated and, as
62 they have a different mode and site of action than the other *Ostreopsis* toxins, their classification as
63 PITX analogues remains uncertain (Mercado et al., 1994; Meunier et al., 1997). To date, the genus
64 *Ostreopsis* comprises eleven species, of which nine have been described by their morphology only,
65 namely *O. siamensis* Johs. Schmidt (Schmidt, 1901), *O. lenticularis* Y. Fukuyo (Fukuyo, 1981), *O.*
66 *ovata* Y. Fukuyo (Fukuyo, 1981), *O. heptagona* D.R.Norris, J.W.Bomber & Balech (Norris et al.,
67 1985), *O. mascarenensis* Quod (Quod, 1994), *O. labens* M.A. Faust & S.L. Morton (Faust and
68 Morton, 1995), *O. belizeana* M.A. Faust, *O. caribbeana* M.A. Faust and *O. marina* M.A. Faust

69 (Faust, 1999), whereas the two most recent descriptions of *O. fattorussoi* Accoroni, Romagnoli &
70 Totti (Accoroni et al., 2016) and *O. rhodesiae* Verma, Hoppenrath & S.A. Murray (Verma et al.,
71 2016) include genetic data. As already reviewed in detail by Parsons et al. (2012), the identification
72 of *Ostreopsis* species based solely on morphology is extremely difficult and many confusions have
73 occurred. Although the generic characters are very peculiar among dinoflagellates and readily
74 identify the genus *Ostreopsis*, the criteria used to delineate species are based primarily on variations
75 in cell size, outline and some slight differences of certain thecal plates (Faust, 1999; Penna et al.,
76 2005; Hoppenrath et al., 2014). However, most of these features have been shown to vary within a
77 given species (e.g. Penna et al., 2005). This significant morphological plasticity thus makes the
78 species identification by morphology often ambiguous (Rhodes et al., 2000; Parsons et al., 2012;
79 Hoppenrath et al., 2014).

80 Owing to the ambiguities in defining the morphological characters, there have been several
81 attempts in revising the description of *Ostreopsis* and species therein, using molecular data (Parsons
82 et al., 2012). To this end, sequences of the Internal Transcribed Spacers (ITS–5.8S rDNA region),
83 or more recently the hypervariable D8–D10 domains of the ribosomal DNA large subunit (LSU
84 rDNA) have been made available for species identification, in combination with morphometrics.
85 One of the first molecular studies on *Ostreopsis* was by Leaw et al. (2001) in Malaysia who showed
86 that within *O. cf. ovata*, the isolates clustered in two distinct clades, corresponding to
87 geographically distinct groups. Later, Penna et al. (2005, 2010) obtained similar results and found a
88 clade of *O. cf. ovata* corresponding to Mediterranean/Atlantic strains, well separated from
89 Indo-Pacific strains. These findings strongly suggest that a given morphospecies can actually
90 encompass a wide genetic cryptic diversity. Studying the genetic diversity of the genus *Ostreopsis*
91 in the western Pacific, Sato et al. (2011) identified 8 clades corresponding to eight putative species,
92 based on two different genetic markers (LSU D8–D10 and ITS–5.8S rDNA sequences). Their
93 molecular data revealed the existence of a new, cryptic species (*Ostreopsis* sp. 1) possessing the

94 same morphology as *O. cf. ovata* and therefore very difficult to describe as a separate species.
95 Moreover, in the absence of reliable genetic references for most of the clades, the authors
96 deliberately did not assign them taxonomically and the different genetic entities were thus named
97 *Ostreopsis* sp. 1–6. Later, Tawong et al. (2014) used the same approach in their analysis of strains
98 from Thailand, and they identified a new genetic clade, *Ostreopsis* sp. 7, for which morphological
99 features cannot be distinguished from *O. cf. ovata*. They concluded that it may represent a yet
100 undescribed cryptic species, but distinctive characters needed to be found to support its description
101 as a separate taxon (Tawong et al., 2014).

102 To date, the taxonomy of *Ostreopsis* is controversial and morphological and molecular data
103 cannot be easily combined in order to delimit species (Hoppenrath et al., 2014). Several genotypes
104 are not yet associated with a morphospecies, leading to a situation of a dual-taxonomy based either
105 on morphospecies or genotypes. In order to unify them, reference molecular data acquired from
106 unambiguously identified specimens are absolutely necessary. Ideally, the genetic data should
107 include type material (holotype, lectotype, neotype), which is the reference point for the application
108 of the species name, according to the International Code of Nomenclature for Algae, Fungi and
109 Plants (Turland et al., 2018). For recently described species (Accoroni et al., 2016; Verma et al.,
110 2016), sequences have been acquired from the same strains as used for the descriptions and thus are
111 taxonomically reliable. In the case of older descriptions without genetic data associated, the
112 situation is more complex since in most cases, the type material has not been designated, is no more
113 available, or, if still extant, has been conserved in an improper way to obtain reliable sequences.
114 Thus, in modern day molecular studies, it is not usually possible or practical to obtain reference
115 sequences from the types, and therefore fresh collections or cultures must be used (Ariyawansa et
116 al., 2014). This creates the problem that sequence data may come from incorrectly named isolates,
117 which can make the whole resulting taxonomy unsound (Ariyawansa et al., 2014). For *Ostreopsis*
118 species, the intraspecific genetic variability is often linked to geographical origins of strains.

119 Therefore, in order to provide reliable information and ensure a correct association between
120 phenotype/genotype of a given species, new investigations and acquisition of reference genetic data
121 should always be made in the type locality.

122 The species *Ostreopsis lenticularis* was first described from Tahiti Island in the Society
123 Archipelago, (French Polynesia), the Gambier Archipelago as well as New Caledonia, by Fukuyo
124 (1981), in the framework of a study of benthic dinoflagellates from coral reefs in the Pacific. This
125 description was based on light microscopy observations. Morphologically, it displays the same size
126 and outline to *O. siamensis* from which it differs by the absence of a body undulation and the
127 presence of two sizes of thecal pores (Fukuyo, 1981; Hoppenrath et al., 2014). Fukuyo (1981) did
128 not designate a holotype, but he indicated that the type locality was Tahiti Island, and that this
129 species was absent in Ryukyu Islands (Japan). Since then, it has been found associated with various
130 benthic habitats in almost all tropical regions in the world (Faust, 1995; Hoppenrath et al., 2014;
131 Gárate-Lizárraga et al., 2018). In some instances, authors identified this species with morphological
132 features different than the ones reported in the original description, which not only makes these
133 reports doubtful but also the species delimitation unclear (e.g. Faust et al., 1996; Leaw et al., 2001;
134 Faust and Gullledge, 2002). In addition, the toxicity status of this species needs to be clarified since
135 no toxicity has been clearly demonstrated in the species described from French Polynesia (Bagnis et
136 al., 1985) whereas several studies from the Caribbean Sea mentioned it as a toxic species (e.g.
137 Mercado et al., 1994). Moreover, from a molecular point of view, the genetic identity of *O.*
138 *lenticularis* appears ambiguous since a sequence ascribed to *O. lenticularis* was identical to another
139 sequence identified as *O. labens*, causing a taxonomic confusion (Penna et al., 2010; Sato et al.,
140 2011). More recently, in the study by Zhang et al. (2018), sequences ascribed to *O. lenticularis*
141 cluster into two separate clades (*Ostreopsis* sp. 5 and *Ostreopsis* sp. 6), making the genetic identity
142 of this species even more elusive. Moreover, Sato et al. (2011) demonstrated that these two clades
143 were genetically divergent enough to support two distinct species and showed that whereas

144 *Ostreopsis* sp. 5 was not toxic to mice, *Ostreopsis* sp. 6 produced ostreocin-D (Suzuki et al., 2012).
145 Hence, the definition of *O. lenticularis* is still unclear and in a context of toxic risks associated with
146 increasing proliferations of *Ostreopsis* species, it is therefore of utmost importance to revisit the
147 taxonomic identity of this species by unambiguously associating phenotypic and genotypic data,
148 and also clarifying its toxic status (Hoppenrath, 2017).

149 The aim of the present study is to re-investigate *O. lenticularis* in the type locality (Tahiti
150 Island) and other sites in French Polynesia, including the Gambier Archipelago mentioned in the
151 original description by Fukuyo (1981). Following recent sampling campaigns conducted in four
152 different archipelagos of French Polynesia, clonal cultures of 47 distinct strains were obtained in the
153 laboratory. The morphology and degree of genetic variation between French Polynesian *O.*
154 *lenticularis* strains were assessed using microscopy analysis and molecular data derived from LSU
155 rDNA (D8–D10) and ITS–5.8S sequences. In addition, the toxic status of 19 of these strains was
156 investigated using the neuroblastoma cell-based assays and, for 4 strains from Tahiti Island, using
157 liquid chromatography coupled with tandem mass spectrometry. All together, these morphological,
158 phylogenetic and toxicological data allowed to refine the descriptive characters of *O. lenticularis*.

159 **2. Material and methods**

160 **2.1 Sampling techniques**

161 Wild samples of *Ostreopsis* were collected from different sites in the Society, Marquesas,
162 Gambier and Australes archipelagos (Fig. 1), using both the natural (i.e., macroalgae) and artificial
163 (i.e., window screens, Ws) substrate methods. Briefly, \approx 200 g of turf-like macroalgae were
164 collected at water depths of 1–5 m and examined for the presence of *Ostreopsis* cells, following the
165 protocol described by Chinain et al. (2010). To this end, macroalgal samples were sealed within
166 plastic bags underwater and shaken and kneaded vigorously to dislodge dinoflagellate cells. The
167 detrital suspension was then successively filtered through 125, 40 and 20 μ m mesh sieves and the

168 40 and 20 μm fractions preserved in 50 mL of 5% formalin-seawater. The artificial substrate
169 method used 150 cm^2 WS devices assembled and deployed for 24 h following the protocol proposed
170 by Tester et al. (2014). After 24 h, WSs were collected with 250 mL of ambient sea water and
171 shaken to dislodge the cells. The entire volume was filtered through 10 μm polycarbonate filters
172 that were replaced as the filters became obstructed. Then, all filters used to process individual
173 samples were transferred to 15 mL tubes with 8 mL of sterile filtered sea water. Before removing
174 the filters, the tubes were shaken to dislodge *Ostreopsis* cells.

175 2.2 *In vitro* culturing of *Ostreopsis*

176 *Ostreopsis* clonal cultures were established from single cells isolated from wild samples, using
177 an inverted microscope. They were routinely maintained in 1 L Fernbach flasks in f10k enriched
178 natural sea water (NSW) medium (Holmes et al., 1991) at 26°C, a salinity of 36, with 7500 lux of
179 light and a 12:12 h light:dark photoperiod. After approximately 21 days of growth, cells were
180 harvested by filtration and centrifugation. Cell counts were achieved using a Coulter counter
181 (Beckman) and the resulting cell pellets lyophilized and weighted. This step was repeated several
182 times for each studied strains, in order to accumulate sufficient cell biomass for further toxicity
183 analysis.

184 A total of 47 strains originating from various locales in French Polynesia (except from the
185 Tuamotu archipelago for which no culture could be established) were analyzed in the present study.
186 All the information relative to these strains, e.g. strain codes, species, year of isolation and location,
187 are summarized in Table 1. These isolates are part of the algal collection of the Laboratory of Toxic
188 Micro-algae of the Institut Louis Malardé (Tahiti, French Polynesia), where cultures are deposited.
189 All the following experiments were conducted on non-axenic acclimated batch cultures.

190 For comparisons with wild cells, subsamples of the WS samples collected in November 2016
191 from Anaho Bay (WS 51.2, 08°49.194'S - 140°03.800'W), Taiohae (WS 55.24, 08°56.009'S -
192 140°05.581'W) and Agapaa (WS 56.14, 08°53.777'S - 140°03.008'W) in Nuku Hiva Island,

193 (Marquesas archipelago) were fixed with acidic Lugol's (for molecular analysis) and 2.5 %
194 glutaraldehyde (for scanning electron microscopy, SEM).

195 *2.3 Microscopy observations*

196 Light microscopy (LM) observations of live cells were conducted using a Leica DMLB
197 microscope (Leica, Wetzlar, Germany) equipped with a D850 DSLR camera (Nikon, Tokyo,
198 Japan).

199 The shape and location of the nucleus were studied in epifluorescence microscopy (EM) after
200 staining cells fixed in ethanol with 1:100,000 SYBR Safe (Thermo Fisher, Waltham, MA, USA). In
201 order to study the thecal plate pattern of the different strains, EM was used after staining
202 Lugol-fixed cells with Solophenyl Flavine 7GFE 500 (Ciba Specialty Chemicals, High Point, NC,
203 USA) according to the method described in Chomérat et al. (2017). The observations were done
204 with a Zeiss Universal microscope fitted with epifluorescence cubes (335WB50 excitation filter,
205 FT395 dichromatic beam splitter and D510/80M emission filter for Sybr Green and 443AF40
206 excitation filter, 475DCLP dichromatic beam splitter, and 500DF25 emission filter for Solophenyl
207 Flavine, Omega Optical, Brattleboro, VT, USA), Nikon CF Fluor optics (Nikon, Tokyo, Japan), an
208 HBO 50-W mercury lamp and a EOS-M digital camera (Canon, Tokyo, Japan).

209 Cells were also observed using field-emission scanning electron microscopy (FE-SEM). Prior
210 to scanning electron microscopy, cells fixed in 2.5% glutaraldehyde from the cultures in early
211 exponential growth phase or the field sample WS 51.2 were first isolated using a micropipette,
212 rinsed in distilled water and processed according to Chomérat and Couté (2008). Dehydration was
213 carried out in ethanol baths of 15%, 30%, 50%, 70%, 95% vol. ethanol, and several baths of
214 absolute ethanol (100%) and then cells were critical point dried using an EMS 850 (Electron
215 Microscopy Sciences, Hatfield, PA, USA) critical point drier. Dried filters were then mounted onto
216 12 mm SEM stubs using carbon adhesive and coated with gold using a Cressington 108Auto
217 (Cressington, Watford, UK) sputter coater. Cells were then observed using a FE-SEM Zeiss

218 SIGMA 300 (Carl Zeiss Microscopy GmbH, Jena, Germany) at the Marine Biology station in
219 Concarneau (France). Measurements were realized directly with the microscope or on digital
220 images using ImageJ software (Rasband, 1997). For measurements of the curved apical pore plate
221 (Po), the arc length was measured in apical view.

222 **2.4 DNA amplification and sequencing**

223 For DNA amplification, direct cell PCR approach was used using one or a few cells from the
224 cultures in early exponential growth phase preserved in ethanol 70%. Under the inverted
225 microscope, fixed cells were pipetted and rinsed in several drops of nuclease-free distilled water,
226 and then transferred into a 0.2 ml PCR tube. A similar process was used for isolation of single-cells
227 from the Lugol-fixed samples from Nuku Hiva.

228 Due to the low amount of DNA, a first round of PCR was realized using ITS-FW and RB
229 primers (Chinain et al., 1999; Nézan et al., 2014), allowing the amplification of the
230 ITS1–5.8S–ITS2 and D8–D10 regions. A second round of PCR (nested PCR) was realized using 1
231 μ l of the amplicon produced in the first step as template. Primers used for the second amplification
232 are given in Chinain et al. (1999) and Nézan et al. (2014), and two internal reverse primers were
233 specifically designed for PCR and sequencing: OstD1R (5'-GTAGCAGCATGCCATGATCA-3')
234 and OstD10R (5'-GCACTGAAAATGAAAATCAAGC-3'). PCR reactions were realized in 20 μ l
235 using KOD Hot Start Master Mix (Novagen-Merck KgaA, Darmstadt, Germany), according to the
236 manufacturer's instructions. The PCR cycling comprised an initial 2 min heating step at 95°C to
237 activate the polymerase, followed by 35 cycles of 95°C for 20 sec, 56°C for 20 s, and a final
238 extension at 70°C for 20 min. Prior to sequencing, amplicons were visualized on an agarose gel
239 after electrophoresis and the positive samples were purified using the ExoSAP-IT PCR Product
240 Cleanup reagent (Affymetrix, Cleveland, OH, USA).

241 The Big Dye Terminator v3.1 Cycle Sequencing Kit (Applied Biosystems, Tokyo, Japan) was
242 used for sequencing of the amplicon generated at the second PCR round. Primers and excess

243 dye-labeled nucleotides were first removed using the Big Dye X-terminator purification kit
244 (Applied Biosystems, Foster City, CA, USA). Sequencing products were run on an ABI PRISM
245 3130 Genetic Analyzer (Applied Biosystems). Forward and reverse reads were obtained. All the
246 information of strains, including origin of sample and accession numbers, are listed in Table 1.

247 ***2.5 Alignment and phylogenetic analyses***

248 For both the D8–D10 and ITS–5.8S rDNA datasets, the 5' and 3' ends were manually aligned
249 to truncate and refine the ends. The D8–D10 dataset was aligned using Clustal Ω v. 1.2
250 implemented in SeaView v. 4.7 (Gouy et al., 2010), while the ITS–5.8S rDNA dataset was aligned
251 using MAFFT algorithm with selection of the q-ins-i strategy (Kato and Standley, 2013). Poorly
252 aligned positions in both alignments were removed using Gblocks algorithm, using less stringent
253 parameters than default (Castresana, 2000).

254 Prior to phylogenetic analyses, the search for the most appropriate model of sequence evolution
255 has been performed using jModeltest2 v. 2.1.7 (Darriba et al., 2012). Two methods of phylogenetic
256 reconstruction were used. Maximum Likelihood analysis (ML) was performed using PHY-ML v. 3
257 (Guindon et al., 2010), and a bootstrap analysis (1000 pseudoreplicates) was used to assess the
258 relative robustness of branches of the ML tree. Bayesian Inference analysis (BI) was realized using
259 MrBayes 3.1.2 (Ronquist and Huelsenbeck, 2003). Initial Bayesian analyses were run with a GTR
260 model (nst = 6) with rates set to gamma. The number of generations used in these analyses was
261 5,000,000 for the LSU rDNA D8–D10 alignment, and 4,000,000 for the ITS–5.8S rDNA alignment,
262 with sampling every 100th generations. The burnin values were set so that the first 10,000 trees were
263 discarded for the LSU rDNA D8–D10, while it was set to 12,000 for the ITS–5.8S rDNA
264 alignment. Therefore, the posterior probabilities of each clade were calculated from the remaining
265 40,000 trees in the LSU analysis, and the remaining 28,000 trees in the ITS–5.8S rDNA analysis.

266 Genetic distance (uncorrected genetic *p* distance) calculations among and within the *Ostreopsis*
267 clades were estimated from the LSU D8–D10 and ITS–5.8S rDNA matrices used for phylogenetic

268 analyses, using the *p*-distance model in MEGA X: Molecular Evolutionary Genetic Analysis across
269 Computing Platforms v. 10.0.5 (Kumar et al., 2018).

270 **2.6 Toxicity analysis**

271 **2.6.1 Extraction procedures**

272 A total of 19 strains were extracted for further toxicity analysis (Table 1). For each strain, 50
273 mg of freeze-dried cells (corresponding to a cell biomass $\geq 10^6$ cells) were sampled and extracted
274 under sonication in 670 μ L of methanol (MeOH)/water (1/1, v/v) for 15 min while cooling the
275 solution in ice. Once cells disruption was completed, the sample was centrifuged at 10,000 g at 4°C
276 for 10 min. The resulting supernatant was carefully recovered and the cell pellet re-extracted twice
277 in 670 μ L of methanol/water (1/1, v/v). All supernatants were then combined (total volume
278 recovered: ≈ 2 mL) and centrifuged at 10,000 g at 4°C for 15 min. Finally, a 1.6 mL aliquot was
279 sampled and stored at -20°C until tested for its toxicity using the neuroblastoma cell-based assay.

280 **2.6.2 Neuroblastoma cell-based assay (CBA-N2a)**

281 The *Ostreopsis lenticularis* cell extracts were analyzed for their toxicity using the
282 neuroblastoma cell-based assay (CBA-N2a), a test designed to detect the presence of PITX-like
283 molecules acting on Na⁺/K⁺-ATPase (Ledreux et al., 2009; Pawlowicz et al., 2013). The procedure
284 for CBA-N2a followed the method previously described by Darius et al. (2018) except that only
285 ouabain was used instead of a mixture of ouabain and veratridine. This assay was first calibrated
286 using a PITX standard purchased from Wako (Ref. 161-26141): the neuroblastoma (neuro-2a) cells
287 were exposed to a serial dilution 1:3 of 9 concentrations of PITX (ranging from 1.5 to 9,524 pg
288 mL⁻¹), in the absence (O⁻ conditions) versus the presence of 250 μ M ouabain (O⁺ conditions) to
289 generate a full dose-response curve. Ten (10) μ L of each concentration were tested in triplicate in
290 O⁻ and O⁺ conditions in three independent experiments. Following 20–22 h incubation period, cell
291 viability was assessed using 3-(4,5-dimethylthiazol-2-yl)-2,5-diphenyl tetrazolium bromide (MTT)

292 assay according to Darius et al (2018). Resulting coloration was measured at 570 nm on a plate
293 reader (iMark Microplate Absorbance Reader, BioRad, Marnes la Coquette, France). Absorbance
294 data were fitted to a sigmoidal dose-response curve (variable slope) based on the 4-parameter
295 logistic model (4PL), allowing the calculation of the concentration causing 50% of maximum
296 cytotoxicity on cell viability (EC_{50}) values using Prism v7.04 software (GraphPad, San Diego, CA,
297 USA).

298 As for the *O. lenticularis* cell extracts, the maximum concentration of extract (MCE) that does
299 not induce unspecific mortality in neuro-2a cells in O^- conditions was established at 23,810 cells
300 equiv. mL^{-1} . As a first screening step, all extracts were tested at this MCE and, if toxic, a full
301 dose-response curve was generated by testing a serial dilution 1:2 of 8 concentrations in the same
302 conditions as for the PITX standard.

303 Finally, the limits of detection (LOD) and quantification (LOQ) of the CBA- N2a test were
304 estimated using the following formula: $LOD = (PITX\ EC_{80}/MCE)$ and $LOQ = (PITX\ EC_{50}/MCE)$.

305 **2.6.3 Liquid Chromatography coupled with tandem Mass Spectrometry**

306 Four strains from Tahiti Island (Table 1), the type locality of *O. lenticularis* were screened for
307 the presence of PITX and related known structural analogues at Ifremer Phycotoxins Laboratory
308 (Nantes, France). Freeze-dried pellets were extracted with methanol (ratio 1:25, weight/volume)
309 using glass beads (250 mg) in a mixer mill (Retsch MM400, Germany) for 20 min at 30 Hz. After
310 centrifugation at 8000 g, supernatants were ultrafiltered (0.20 μm , Nanosep MF, Pall, Mexico)
311 before LC-MS/MS analyses. Liquid chromatography was performed on a Poroshell 120 EC-C18
312 column (100 \times 2.1 mm, 2.7 μm , Agilent, France) equipped with a guard column (5 \times 2.1 mm, 2.7
313 μm , same stationary phase) using a Nexera Ultra-Fast Liquid Chromatography system (Prominence
314 UFLC-XR, Shimadzu, France). Gradients of water (A) and acetonitrile 95% (B) both containing
315 0.2% of acetic acid were used at a flow rate of 0.2 $mL\ min^{-1}$. Injection volume was 5 μL and

316 column temperature 25 °C. MS/MS analyses were performed with an API 4000QTRAP (AB Sciex,
317 France) in positive ion mode and using MRM (Multiple Reaction Monitoring) acquisition. UV
318 detection at 220, 233, 263 and 220-360 nm was performed with a diode array detector (Prominence,
319 SPD-M20A, Shimadzu, France). In total, two LC-MS/MS and one LC-UV-MS/MS methods (Table
320 S1) were used to detect PITX, 42-OH-PITX, 12 OvTXs (-a to -k), OST-B and -D, 3 McTXs (A to
321 C) and OTX-1 and -3 (Table S1). Quantification was performed relative to Palytoxin standard
322 (Wako Chemicals GmbH, Germany) with a 6-point calibration curve. Limit of detection and
323 quantification were 20 and 30 ng mL⁻¹ for PITX standard.

324 **3. Results**

325 **3.1 Microscopy observations**

326 Observations in light and epifluorescence microscopy of the 47 strains analyzed in the present
327 study revealed similar morphological features. The cells were broadly oval in shape, lenticular and
328 photosynthetic, as shown for the strain THT16–4 (Fig. 2A). The oval nucleus was located dorsally
329 (Fig. 2B). A similar thecal plate pattern has been observed in all the strains. For this reason, only the
330 epifluorescence micrographs of one strain from each archipelago and wild specimens from a WS
331 sample are presented in Fig. 3, for comparison purpose. No morphological difference could be
332 observed among the strains and field specimens from the different archipelagos (Figs 3A-O), and all
333 the features identify the species *Ostreopsis lenticularis*.

334 For a detailed morphological analysis, the strain THT16–4 from Tahiti Island (Society
335 Archipelago) has been chosen for further investigations using FE-SEM. Scanning electron
336 micrographs of one strain from Australes, Marquesas and Gambier archipelagoes are given in
337 supplementary figure S1. Additionally, for comparison, cells from the field sample WS 51.2 from
338 Nuku Hiva Island (Marquesas Archipelago) were also used for a detailed observation of wild
339 specimens corresponding to the same morphotype.

340 *3.1.1 Culture THT16–4 from Tahiti Island*

341 Specimens were broadly oval in apical and antapical views (Figs 2A, 3A-B, 4A-B). The cells
 342 were biconvex, and flattened, with the cingulum straight in lateral view (Figs 4C-D). They were
 343 60.5–89.3 μm (mean 80.3 μm ; s.d. 7.5 μm , $n = 30$) deep (dorso-ventral length) and 56.1–73.4 μm
 344 (mean 65.8 μm ; s.d. 5.4 μm , $n = 30$) wide. The DV/W ratio was 1.08–1.36 (mean 1.22; s.d. 0.08, n
 345 = 27).

346 The thecal plate pattern was APC 3' 7'' 6c 4?s 5''' 2''''', and thecal plates were clearly visible
 347 both with light epifluorescence microscopy and SEM (Figs 3A-B, 4A-D, 5A-C). The apical pore
 348 complex (APC) consisted in a narrow, elongated and slightly curved Po plate bearing a slit and two
 349 rows of pores (Figs 5A-B). It was located parallel to the left mid-lateral to dorsal cell margin. The
 350 Po plate was 16.2–19.3 μm (mean 17.4 μm ; s.d. 0.8 μm , $n = 15$) long. The first apical plate (1') was
 351 elongated, located mostly on the left side of the cell (Fig. 4A). On its dorsal part, it is slightly
 352 protruding over the APC (Figs 4A, 5A). The second apical plate (2') was narrow and elongated, and
 353 located below the APC, extending dorsally the Po plate, and reaching about the mid-position of the
 354 3' plate (Figs 3C, 4D, 5A-B). The third apical plate (3') plate was hexagonal in shape, in contact
 355 with 1', 2', 3'', 4'', 5'' and 6'' but also had a very short suture with Po (Figs 4A, 5A-B). In the
 356 precingular series, 1'' was the smallest while 6'' was the largest (Figs 3A, 4A). All precingular
 357 plates were four-sided except 2'' and 6'' that were pentagonal (Fig. 4A). The cingulum was narrow
 358 and straight (Figs 4C-D). The postcingular plate series comprised 5 plates (Figs 3B, 4B-C), 1'''
 359 being small and more conspicuously visible in ventral view than in antapical view (Fig. 4C). The
 360 remaining four postcingular plates were large (Fig. 4B). Among postcingular plates, 1''' was
 361 three-sided (Fig. 4C), 2''' five-sided, and 3''', 4''' and 5''' four-sided (Figs 4B, 6B). The two antapical
 362 plates were unequal in size, 1'''' being relatively small and in contact with the cingulum and the left
 363 side of the posterior sulcal plate (Sp), while 2'''' was elongated, with its sutures with 2''' and 5'''
 364 nearly parallel (Figs 3B, 4B).

365 The cingulum consisted of 6 distinct plates (supplementary Fig. S2). The sulcus was not
366 studied in detail and only four plates were observed, with Sp being roughly pentagonal, Sda having
367 a conspicuous list, Ssa partially hidden by overlapping 1'''' (Fig. 5C). Another plate, only partially
368 visible, was present between Sp and Sda (Fig. 5C). The presence of other platelets could not be
369 revealed from the observations.

370 The thecal surface was smooth and plates possessed numerous pores of two kinds. Large pores
371 were round, 0.29 – 0.59 μm in diameter (mean 0.41 μm ; s.d. 0.08 μm ; $n = 60$),) and scattered all
372 over the plates. Rarely, they were oblong to elongated in some plates of the theca, as in the 1'''' ,
373 while other plates have round pores (Fig. 5C). Small pores, 75–120 nm in diameter (mean 102 nm;
374 s.d. 13 nm; $n = 70$) were abundant and scattered on the surface of thecal plates (Fig. 5D) but due to
375 their small size, they could be observed only at high magnifications in LM and epifluorescence, and
376 with SEM (Figs 3C, 5D).

377 **3.1.2 Wild specimens collected from window-screen samples**

378 Cells were large, subcircular in shape, slightly pointing ventrally (Figs 3N-O, 6A-B). They
379 were biconvex and flattened (Figs 6C-D), 73.0–94.4 μm in dorso-ventral length (mean 81.2 μm , s.d.
380 5.7 μm , $n = 22$) and 58.0–78.2 μm in width (mean 67.5 μm , s.d. 6.1 μm , $n = 22$). The DV/W ratio
381 was 1.08–1.32 (mean 1.21; s.d. 0.01, $n = 22$).

382 The thecal pattern was APC 3' 7'' 6c 4?s 5''' 2'''' (Figs 3N-O, 6A-F), and all plates were found
383 to possess the same characteristics than previously described for the strain THT16–4 (Figs 6A-G).
384 As for the cells in culture, specimens from the field sample were smooth and possessed two kinds of
385 thecal pores: large pores were round, 0.4 μm in diameter, and smaller pores (ca. 0.1 μm) were
386 abundant and scattered all over the surface of the theca (Fig. 6G). With high resolution SEM, no
387 morphological difference was found among field specimens and those from the culture THT16–4.

388 3.2 Molecular phylogenies

389 3.2.1 LSU rDNA D8–D10 regions

390 In the phylogenetic analysis inferred from LSU D8–D10 sequences, 50 new sequences
391 acquired from French Polynesia (from 47 strains in culture and 3 single-cells isolated from a field
392 sample from Nuku Hiva Island), with reference sequences retrieved from GenBank, were used. The
393 final alignment comprised 110 sequences and had a length of 696 base pairs, with 174 variable
394 sites, of which 114 were parsimony informative. The best-fit model of LSU D8–D10 sequences was
395 found to be TN93 + *I* + *G* model with the following parameters: Ti/Tv for purines = 2.312, Ti/Tv
396 for pyrimidines = 5.531, base frequencies of *A* = 0.28009, *C* = 0.17427, *G* = 0.24939, *T* = 0.29625;
397 assumed with invariable sites (*I* = 0.503) and gamma distribution shape (*G* = 0.512).

398 Both analyses performed with ML and BI gave the same tree topology and the relationships
399 among *Ostreopsis* clades were identical. Hence, only the majority-rule consensus tree of the ML
400 analysis is shown (Fig. 7). The tree shows that there are ten distinct clades (*O. cf. ovata*, *O. cf.*
401 *siamensis*, *O. rhodesiae* and *Ostreopsis* spp. 1–7 clades). All sequences of *O. lenticularis* acquired
402 in this study from various sites in French Polynesia cluster with a strong support in a monophyletic
403 group comprising also three strains from Okinawa and Iriomote Islands in Japan (s0577, s0578 and
404 IkeOst2) and previously assigned to *Ostreopsis* sp. 5 by Sato et al. (2011) (Fig. 7). This clade
405 appears to be sister with a group of ten sequences from Shikoku Island (Japan) also previously
406 ascribed to *Ostreopsis* sp. 5 (Fig. 7). Because of their low divergence (*p*-distance between the
407 groups of 0.010, Table 2), these two groups are considered as two subclades of *O. lenticularis* (=
408 *Ostreopsis* sp. 5).

409 Results of the phylogenetic analysis showed that *O. lenticularis* is a sister to *Ostreopsis* sp. 6
410 with maximal support (ML = 100, BI = 1.00). The clade *Ostreopsis* sp. 6 is divided into three
411 subclades, one including four sequences from Japan (IR33, IR49, OU8, OU11), one including two

412 sequences from Japan (s0587 and s0595) and one two sequences from Thailand (TF25OS,
413 TF29OS) (Fig. 7). The *p*-distance between these subclades in *Ostreopsis* sp. 6 ranged from 0.014 to
414 0.020 (Table 2).

415 3.2.2 ITS–5.8S rDNA phylogeny

416 In the phylogenetic analysis inferred from ITS–5.8S rDNA sequences, we used 19 new
417 sequences acquired from French Polynesian strains with other sequences retrieved from GenBank.
418 The final alignment comprised 92 sequences and had a length of 329 base pairs, with 222 variable
419 sites, of which 175 were parsimony informative. The best-fit model of ITS–5.8S rDNA sequences
420 was found to be TN93 + *G* model with the following parameters: Ti/Tv for purines = 9.128, Ti/Tv
421 for pyrimidines = 0.148, base frequencies of A = 0.27149, C = 0.19120, G = 0.18559, T = 0.35172;
422 assumed with a gamma distribution shape (*G* = 0.636).

423 Both analyses performed with ML and BI gave the same tree topology and the relationships
424 among *Ostreopsis* clades were identical. Hence, only the majority-rule consensus tree of the ML
425 analysis is shown (Fig. 8). The tree shows that there are twelve distinct clades (*O. cf. ovata*, *O. cf.*
426 *siamensis*, *O. fattorussoi*, *O. rhodesiae*, and *Ostreopsis* spp. 1–8 clades). All sequences of *O.*
427 *lenticularis* acquired in this study from various sites in French Polynesia cluster with a strong
428 support in a monophyletic group comprising also eight sequences from Réunion Island, China,
429 Hawaii and Galapagos Islands, and a subclade of three sequences from Japan (Shikoku Island) (Fig.
430 8). These sequences were previously ascribed to *Ostreopsis* sp. 5 (strains MB80828-4, O70421-1,
431 O70421-2), *Ostreopsis* sp. (isolates P-079.1L, P-079.2L, P-0107, P-0108, P-0109, strain
432 CBA0203), *O. cf. lenticularis* (isolate 17G) and only the strain 2S1E10 was identified as *O.*
433 *lenticularis* in GenBank. The sequences from the Pacific Ocean, Indian Ocean and South China Sea
434 are genetically very closely related (*p*-distance within the clade 0.001, Table 3) but they are slightly

435 divergent from the three sequences from Japan (p -distance between the subclades of 0.068, Table
436 3).

437 In the phylogenetic analysis, *O. lenticularis* is a sister to *Ostreopsis* sp. 6 with good support
438 (ML = 84, BI = 0.96, Fig. 8). Nine sequences from various localities of Southeastern Asia and
439 Japan cluster within this clade. The two sequences FM244728 from Malaysia (ascribed to *O.*
440 *labens*) and AF218465 (ascribed to *O. lenticularis*) cluster together and are identical (Table 3). Two
441 sequences from the Gulf of Thailand AB841254 and AB842255 (ascribed to *Ostreopsis* sp.) and
442 two sequences from Japan (IR33 and OU11) form a sister clade to the Malaysian sequences (Fig. 8).
443 The sequence s0587 is basal to these sequences and its distance varied from 0.110 to 0.161 (Table
444 3). Two sequences from Vietnam diverge earlier in the *Ostreopsis* sp. 6 clade and their genetic
445 distances with all other sequences of the clade varied from 0.057 to 0.135 (Table 3).

446 3.3 Toxicity assessment

447 3.3.1 CBA-N2a analysis

448 The EC₅₀ values for PITX in O⁻ and O⁺ conditions were $1,191 \pm 175 \text{ pg mL}^{-1}$ ($n = 3$) and $107 \pm$
449 36 pg/mL ($n = 3$), respectively. The LOD was estimated at 44.3 ± 4.7 and $3.4 \pm 1.5 \text{ fg PITX}$
450 equiv./cell in O⁻ and O⁺ conditions, respectively, whereas LOQ was estimated at 50 ± 7.3 and $4.5 \pm$
451 $1.5 \text{ fg PITX equiv./cell}$ in O⁻ and O⁺ conditions, respectively.

452 For all the samples tested, no toxicity was detected at the MCE.

453 3.3.2 LC-UV-MS/MS analysis

454 In the four tested strains originating from Tahiti Island analyzed, all the 21 toxic compounds
455 that were targeted were below detection levels.

456 4. Discussion

457 4.1 Morphological features

458 All the strains observed in this study displayed a similar morphology and no difference was
459 observed between specimens from cultures and from field samples. Morphologically, the broadly
460 oval shape, size range, and thecal plate pattern displayed by all the specimens from field samples
461 and strains from widely distant islands were in perfect agreement with the original description of *O.*
462 *lenticularis* by Fukuyo (1981), who reported it from French Polynesia (Tahiti Island as type
463 locality). As mentioned by Fukuyo (1981), the cingulum was not undulated and cells possess two
464 different sizes of thecal pores. The presence of both small and large pores on thecal plates was
465 conspicuous in all specimens examined, even at high magnification with epifluorescence
466 microscopy. Interestingly, in *O. lenticularis*, the smaller pores were much more abundant than
467 larger pores, a feature not reported from any other known species. Indeed, the presence of smaller
468 pores less abundant than larger pores has been reported in *O. rhodesiae*, but they were rare (Verma
469 et al., 2016). Zhang et al. (2018) reported the presence of small, large and also oblong to
470 kidney-shaped pores as a third type of pores present in the strains from Hainan Island (China). In
471 the present study, oblong pores were observed in some *O. lenticularis* specimens in culture, but this
472 was uncommon and only located on some plates of the theca. Such pores were not found in any of
473 the specimens from the field samples. It should be noted that Zhang et al. (2018) reported very large
474 sizes for some specimens (up to 121.3 μm in DV) that were larger than in the original description,
475 and the presence of oblong pores may be related to the size and age of the specimens. This feature
476 should be carefully checked in further studies as it likely results from morphological plasticity and
477 an extreme variation of the large pores. Since the specimens from China were genetically almost
478 identical to those from French Polynesia, this feature may not be taxonomically significant.
479 Contrary to Zhang et al. (2018) conclusions, it is suggested that the presence of two sizes of thecal

480 pores is actually a stable character in *O. lenticularis*, as it was conspicuous in all the specimens
481 examined in French Polynesia and Tahiti (type locality).

482 **4.2 Comparison of *O. lenticularis* to other broadly oval species**

483 As previously reported by Hoppenrath et al. (2014), *O. lenticularis* shares most of its
484 morphological features (e.g. size, outline shape, and thecal plate pattern) with *O. siamensis*. The
485 more or less elongated or round shape cannot be used to differentiate these species (Hoppenrath et
486 al., 2014). In his description of the genus and type species *O. siamensis*, Schmidt (1901)
487 emphasized morphological characters such as flattening of the cell, oyster-shape, short sulcus, and
488 thecal plate pattern (Schmidt, 1901) which define well the genus but are shared by almost all the
489 species (Parsons et al., 2012). The size of *O. siamensis* (dorso-ventral length) is about 90 μm , the
490 theca possesses conspicuous pores and, from the illustration, *O. siamensis* has a body undulation,
491 visible in lateral view (Schmidt, 1901). According to Fukuyo (1981), *O. lenticularis* differs from *O.*
492 *siamensis* by the absence of a body undulation and by the presence of fine pores densely scattered
493 all over the thecal plates, which is also observed for all the specimens examined herein. Some
494 authors (e.g. Penna et al., 2005; Parsons et al., 2012) claimed that Fukuyo used the difference in cell
495 shape to distinguish *O. siamensis* from *O. lenticularis*, but this statement is erroneous since Fukuyo
496 (1981, pp. 970-971) clearly indicated a similar size and outline for these two species, and mentioned
497 the shape only to distinguish *O. lenticularis* from *Gambierdiscus toxicus*. In the Ryukyu Islands,
498 Fukuyo (1981) identified specimens with a body undulation and only one type of thecal pores, and
499 ascribed them to *O. siamensis*. The author mentioned the absence of this morphotype in the French
500 Polynesian and New Caledonian samples that he studied (Fukuyo 1981), a statement that could be
501 confirmed in the present study.

502 Despite Fukuyo's very clear interpretation (Fukuyo 1981), the distinction between *O.*
503 *lenticularis* and *O. siamensis* based on thecal pores and undulation of the cingulum did not gather
504 consensus among taxonomists. For instance, Norris et al. (1985) questioned this interpretation and

505 regarded *O. lenticularis* as being conspecific with *O. siamensis* rather than as an independent
506 species. At the same period, a series of confusing identifications were made in the Caribbean area.
507 Carlson (1984) identified *O. siamensis* as a relatively rare species around Virgin Islands, although
508 dominant in some stations, but he also emphasized that the distinction between this species and *O.*
509 *lenticularis* was questionable for some specimens. On the following year, Carlson and Tindall
510 (1985) changed this identification to *O. lenticularis* using the same dataset, which added to the
511 confusion. Working on the south west coast of Puerto Rico, Ballantine et al. (1985) initially
512 mentioned *Ostreopsis* sp., but it was then renamed *Ostreopsis* cf. *lenticularis* (Tosteson et al., 1986)
513 and later *O. lenticularis* (Ballantine et al., 1988; Tosteson et al., 1989), thus emphasizing the doubt
514 regarding the identification of this species. Later, Faust et al. (1996) confused even more the
515 taxonomy by reporting the presence of *O. lenticularis* with a morphological description which does
516 not support this identification (only one size of thecal pores). Conversely, in the same study, *O.*
517 *lenticularis* was likely misidentified as “*O. siamensis*” since the morphology (size and two sizes of
518 thecal pores) was in agreement with the original description by Fukuyo (1981). As already pointed
519 out by several authors (Penna et al., 2012; Hoppenrath et al., 2014; Gárate-Lizárraga et al., 2018),
520 these erroneous interpretations were a major source of confusion in the delineation of both *O.*
521 *siamensis* and *O. lenticularis* for subsequent workers. For instance, reports of *O. lenticularis*
522 showing different features than the ones provided in the original description (e.g. Chang et al.,
523 2000; Leaw et al., 2001) appear doubtful and likely correspond to misidentifications of other
524 *Ostreopsis* species rather than reflecting a true variability in *O. lenticularis*.

525 Confusions with other broadly oval species may also have occurred with two additional species
526 with a similar shape to *O. siamensis* and *O. lenticularis*, and overlapping sizes. Faust and Morton
527 (1995) described *O. labens* from Belizean and Japanese samples. This species possesses only one
528 type of pore (trichocyst pores) conspicuously visible in LM, showing an average diameter of 0.3 μm
529 (Faust and Morton, 1995). Later, Faust (1999) described *O. marina*, another species in the same

530 size-range and a roughly oval shape. It is described with a longer Po plate (24 μm vs. 18 μm in *O.*
531 *labens*) and only “minute pores visible only by SEM or epifluorescence microscopy” whose size
532 (0.33 μm , Faust 1999) is larger than in *O. labens* (0.3 μm , Faust and Morton 1995) for which pores
533 were described as conspicuous in LM (Faust and Morton, 1995). These contradictory statements
534 added to the taxonomic confusion, and additionally, *O. marina* has not been compared with *O.*
535 *labens* in the description (Faust 1999).

536 Although Gárate-Lizárraga et al. (2018) consider that these four large and oval species are
537 ‘readily distinguishable by their plate pattern’, their delimitation remains unclear owing to the
538 existing variability in the thecal plates pattern of *Ostreopsis* species along with their poor
539 descriptions (Hoppenrath et al., 2014). The length of certain thecal plates such as Po might be a
540 weak character to distinguish among them. To date, *O. labens* and *O. marina* should be considered
541 as doubtful species for which further studies are necessary not only to prove their existence but also
542 to provide reliable morphological and molecular characters useful for their discrimination from *O.*
543 *siamensis*. In all cases, these three species were all described showing only one kind of thecal pore,
544 and therefore no confusion is possible with *O. lenticularis* which can be easily distinguished from
545 all other known *Ostreopsis* species.

546 **4.3 Molecular phylogenies and taxonomic implications**

547 The molecular phylogenies inferred from this study reveal that all the large and oval specimens
548 identified as *O. lenticularis* in all the study sites from French Polynesia are genetically identical and
549 belong to a unique genotype, previously found in the Pacific close to Japan and named ‘*Ostreopsis*
550 sp. 5’ by Sato et al. (2011) and subsequent authors. This finding of only one genotype in all study
551 sites confirms that the same species is widespread in the different archipelagos of French Polynesia
552 and supports Fukuyo’s former observations of *O. lenticularis* in the Society and Gambier
553 Archipelagos (Fukuyo, 1981). This situation corresponds to the scenario 1 described in Sato et al.
554 (2011), and since morphological and molecular data are congruent, it is straightforward to assign

555 taxonomically the genotype *Ostreopsis* sp. 5 to *O. lenticularis*. This result confirms the
556 identification by Zhang et al. (2018) of specimens from Hainan Islands, but it also highlights the
557 misidentification of some sequences annotated as *O. lenticularis* in GenBank. To date, about fifteen
558 sequences of various genetic markers (rDNA, ITS regions, *cox1*) have been ascribed to *Ostreopsis*
559 *lenticularis* in GenBank, coming from various areas: Portugal, Malaysia, China and Viet Nam but
560 none was acquired in the type locality (Tahiti Island) or in French Polynesia. As previously shown
561 by Sato et al. (2011), some of these sequences clustered with *Ostreopsis* sp. 6, which is genetically
562 divergent enough to be regarded as a separate species from *Ostreopsis* sp. 5 (Sato et al., 2011; this
563 study). For instance, the sequences AF218465 (strain O1PR01 from Malaysia) ascribed to *O.*
564 *lenticularis* and the sequence FM244728 annotated as *O. labens* cluster with *Ostreopsis* sp. 6,
565 proving an identification issue (Penna et al., 2010; Sato et al., 2011). For the strain OPR01 from
566 Malaysia, morphological features such as ‘trichocysts pores equal in size’ reported by Leaw et al.
567 (2001) contradict with Fukuyo’s original description of *O. lenticularis* and suggest a
568 misidentification. Hence, the identity of the specimens clustering within *Ostreopsis* sp. 6 should be
569 re-evaluated as, morphologically speaking, this clade corresponds to a large and lenticular species
570 with thecal pores of one size only, such as *O. siamensis* (*sensu* Fukuyo 1981), *O. labens* or *O.*
571 *marina* (Faust and Morton 1995, Faust et al. 1996).

572 In order to resolve the taxonomic assignment of *Ostreopsis* sp. 6, reference sequences from the
573 type localities of these species are necessary for comparisons, but none are currently available.
574 Nevertheless, Tawong et al. (2014) recently sampled several sites in the Gulf of Thailand, including
575 one site (TF) located on the north coast of the small Koh Wai Island, off the south of Koh Chang
576 Island. Interestingly, this location is close to the sites where *O. siamensis* was originally described
577 by Schmidt (1901) (stations 3 and 6, south of Koh Chang, while the station 2, between Koh Kahdat
578 and Koh Kut was about 15-20 km southeast). Because of this close proximity, this area could be
579 considered as the type locality of *O. siamensis* even if it was not formally designated as such. In

580 contrast with Schmidt (1901) who found only one morphotype (large and oval cells) in plankton
581 samples, Tawong et al. (2014) found two different species in the site TF, *O. cf. ovata* (South China
582 subclade) which is ovate and rather small, and large oval cells with a typical undulation of the
583 cingulum (*Ostreopsis* sp. 6, strain TF29OS). When observed with epifluorescence microscopy,
584 these large specimens were found to have only one size of thecal pores (Tawong et al., 2014) but
585 this was not further confirmed by SEM observations. Genetically, the strains TF29OS and TF25OS
586 are closely related to the sequence of the Malaysian strain O1PR01, possessing similar
587 morphological features and only one type of thecal pores (Leaw et al., 2001). Results of the
588 phylogenetic analysis conducted in the present study clearly confirm that these three strains rather
589 belong to *Ostreopsis* sp. 6, and are not related to *O. lenticularis* as speculated by Zhang et al.
590 (2018), in absence of reference sequence from Tahiti Island for this species. The morphological and
591 molecular studies by Leaw et al. (2001) and Tawong et al. (2014) are congruent to associate
592 specimens with only one size of thecal pores and a body undulation with *Ostreopsis* sp. 6.
593 Interestingly, these morphological features are in perfect agreement with Schmidt's description and
594 illustrations of *O. siamensis* (Schmidt, 1901), and the area where *Ostreopsis* sp. 6 has been found
595 (TF site), coincides with the type locality of this species. Hence, it can be hypothesized that
596 *Ostreopsis* sp. 6 likely corresponds to *O. siamensis* as it was the unique large oval species with all
597 the morphological characters of this taxon found in the type locality. The environment and species
598 composition in this area could have changed during more than a century, but in the absence of
599 Schmidt's original material available, a complete re-investigation of specimens from this locality in
600 the Gulf of Thailand and the designation of an epitype of *O. siamensis* would indisputably stabilize
601 the taxonomy of this complicated genus for which several confusions occurred in the past
602 (Ariyawansa et al., 2014).

603 As emphasized by Tawong et al. (2014), no sequence from the Gulf of Thailand clustered in
604 the clade '*O. cf. siamensis*' in the phylogenies. A similar result has been found in the present study,

605 but since all the sequences of this clade were obtained from subtropical regions of Europe (Portugal,
606 Spain, Italy) and New Zealand (Kerikeri, northern part of North Island), all very distant from the
607 type locality (Gulf of Thailand) located in the tropical area, their taxonomic assignation should be
608 considered with care. As already suggested by Penna et al. (2010), the specimens of the '*O. cf.*
609 *siamensis*' clade likely correspond to another separate taxon, provided a proper description is
610 proposed.

611 Based on the present study conducted in the type locality of *O. lenticularis*, molecular
612 comparisons show that specimens from the Gulf of Thailand and French Polynesia are clearly
613 distinct, supporting Fukuyo's interpretation of *O. siamensis* and the description of *O. lenticularis* as
614 a separate species. Similar investigations in the type localities of *O. labens* and *O. marina* are
615 absolutely necessary to support that they are genetically distinct, since they are very difficult to
616 separate from *O. siamensis* from a morphological point of view.

617 **4.4 Biogeography of *O. lenticularis***

618 In his description, Fukuyo (1981) reported the presence of *O. lenticularis* not only in Tahiti
619 Island, but also Gambier Archipelago and New Caledonia, which indicates a wide distribution
620 within the tropical Pacific Ocean. This study confirms the wide presence of this species in four
621 archipelagos of French Polynesia, and the phylogenetic analysis also confirms the presence of *O.*
622 *lenticularis* in other locations of the Pacific including Japan (Iriomote, Okinawa, Shikoku Islands),
623 Hawaii and Galapagos Islands. Interestingly, Fukuyo (1981) did not observe *O. lenticularis* but *O.*
624 *siamensis* in the Ryukyu Islands whereas Sato et al. (2011) found mixed populations of *O.*
625 *lenticularis* (as *Ostreopsis* sp. 5) and *Ostreopsis* sp. 6. in Okinawa and Iriomote Islands, in the
626 southern subtropical part. At the scale of the Pacific, *O. lenticularis* has a wide distribution, from
627 the temperate Japan to the tropical Pacific while *Ostreopsis* sp. 6 is absent from French Polynesia
628 and may be more restricted to the subtropical area, as suggested by Sato et al. (2011). Despite the
629 lack of molecular support, the identification of *O. lenticularis* in Revillagigedo archipelago by

630 Gárate-Lizárraga et al. (2018) is well supported by morphological features, and consistent with the
631 finding of this species in Galapagos Islands in the eastern Pacific.

632 In the western Pacific, molecular data confirm the presence of this species in the China Sea
633 (Zhang et al., 2018) but not in Malaysia and Thailand where previous reports probably correspond
634 to misidentifications of *Ostreopsis* sp. 6 (e.g. Leaw et al. 2001). Unambiguous report of *O.*
635 *lenticularis* in Vietnamese waters, based on detailed morphological identifications showing the two
636 types of thecal pores was also provided by Larsen and Nguyen Ngoc (2004). These authors also
637 found another large oval species with one type of thecal pores, and a long Po plate (24 μm) which
638 they ascribed to *O. marina* and did not report *O. siamensis* (Larsen and Nguyen Ngoc, 2004).
639 Molecular studies would be necessary for a better characterization of the latter species.

640 In the Indian Ocean, the presence of *O. lenticularis* around La Réunion Island was mentioned
641 by Hansen et al. (2001). In their study, Carnicer et al. (2015) recorded large specimens difficult to
642 assign to a species by morphology because they appeared close to *O. siamensis* and *O. lenticularis*,
643 although their size that better fit *Ostreopsis marina*. Unfortunately, no detailed observations with
644 SEM were performed and the presence of one or two kinds of pores was not clearly demonstrated
645 by epifluorescence microscopy. Genetically, these specimens were found to belong to *Ostreopsis*
646 sp. 5 (Carnicer et al., 2015) and, based on the present study, are genetically identical to *Ostreopsis*
647 *lenticularis* from French Polynesia. Hence, the presence of this species in southwestern Indian
648 Ocean is confirmed by molecular data. Since all the sequences obtained by Carnicer et al. (2015)
649 are closely related and belong to *O. lenticularis*, the record of *O. marina* (as a paratype) in Mayotte
650 Island (south west Indian Ocean) by Faust (1999) remains in question owing to the very similar size
651 and morphology between these two species. Nevertheless, further molecular studies are necessary in
652 the Indian Ocean since Hansen et al. (2001) also reported the presence of *O. siamensis*.

653 In the Caribbean, *O. lenticularis* has been reported on several occasions (e.g. Ballantine et al.,
654 1985; Carlson and Tindall, 1985; Faust, 1995; Delgado et al., 2006; Marchan-Álvarez et al., 2017)

655 but all the identifications were based on morphological observations only, which caused some
656 confusions as emphasized in section 4.2. As seen in Tindall et al. (1990), Faust et al. (1996) and
657 Faust and Gullede (2002) studies, several species very similar in shape and size did co-occur in
658 this area, but specimens morphologically identical to *O. lenticularis* were reported, suggesting the
659 likely presence of this species in the dinoflagellate assemblages.

660 From all these observations, it can be concluded that *Ostreopsis lenticularis* is widely
661 distributed in the tropical areas of the world oceans but to date, molecular data supporting its
662 identification are still lacking from the Caribbean Sea and the Atlantic Ocean.

663 **4.5 Toxicity assessment**

664 All 19 strains of *Ostreopsis lenticularis* tested for their toxicity using the CBA-N2a showed no
665 toxic activities on neuroblastoma cells. Likewise, neither PITX-like compounds nor OTX-1 and
666 OTX-3 were detected in any of the 4 extracts analyzed by LC(-UV)-MS/MS, which is consistent
667 with Sato et al. (2011) who previously observed no toxic effect on mice in *Ostreopsis* sp. 5 (now
668 identified as *O. lenticularis*) extracts. Contrastingly, these authors reported that *Ostreopsis* sp. 6
669 was toxic to mice and, more specifically, mentioned the detection of OST-D in strain s0587 extract
670 (Sato et al., 2011), although some strains genetically distinct (OU11, IR33) of this species did not
671 produce this compound (Suzuki et al., 2012). Overall, these findings highly support the idea that
672 *Ostreopsis lenticularis* and *Ostreopsis* sp. 6 correspond to two different species.

673 The present results may appear contradictory with previous studies mentioning the toxicity in
674 *O. lenticularis* strains from the Caribbean area (Lassus et al., 2016). These data should be
675 considered cautiously since the identification of the toxic species was not clear. The first toxic
676 effect on mice associated with *O. cf. lenticularis* was reported by Tosteson et al. (1986) but without
677 any taxonomical assessment of the species. Ballantine et al. (1988) mentioned higher toxicity levels
678 in strains of '*O. lenticularis*' from the Caribbean as compared to those from Tahiti localities where
679 this species was found in abundance but not obviously toxic according to Bagnis et al. (1985).

680 Ballantine et al. (1988) explained this apparent discrepancy by the use of different extraction
681 methods but, surprisingly, did not question the taxonomic identification of the species. Tindall et al.
682 (1990) further performed a taxonomic investigation on the toxic clones from the Caribbean and
683 observed that (i) the cells size range was compatible with both *O. siamensis* and *O. lenticularis*, and
684 (ii) cells had an undulating cingulum and one type of thecal pores. Although these features should
685 have definitely excluded *O. lenticularis*, these authors kept using the name *O. lenticularis* under the
686 pretext that *O. siamensis* had never been reported from the Caribbean (Tindall et al., 1990), thus
687 perpetuating the confusion. It was yet rather clear that another species than *O. lenticularis* was the
688 toxic species producing the water soluble ostreotoxins (OTXs) inhibiting the acetylcholine response
689 (Tindall et al., 1990). Several subsequent studies investigated the mode of action of the toxic
690 compounds and effects of bacteria on the toxicity of *Ostreopsis* strains from the Caribbean
691 designated doubtfully as '*O. lenticularis*' (Mercado et al., 1994, 1995; Meunier et al., 1997;
692 Pérez-Guzmán et al., 2008), but in their review, Parsons et al. (2012) highlighted the fact that these
693 reports of toxic strains of *O. lenticularis* in the Caribbean were subject to caution, and purposely
694 used quotations marks.

695 From the present study, it appears more likely that the toxic strains formerly assigned to the
696 species *O. lenticularis* were, in fact, misidentified due to morphological confusions and the lack of
697 molecular data to confirm such identifications. Further studies using molecular techniques to
698 characterize these toxic strains are needed to clarify this point. So far, in light of the present
699 findings, there is still no true evidence for the existence of toxic strains in the species *O.*
700 *lenticularis*, which raises the question of the relevance of keeping this species in the IOC-UNESCO
701 taxonomic reference list of harmful micro-algae (Akselman and Fraga, 2018).

702 ***4.6 Lectotype designation***

703 When describing *O. lenticularis* from Tahiti Island, Fukuyo (1981) did not designate a
704 holotype associated with the name, but provided five LM pictures and two interpretation drawings.

705 From the analysis conducted on several culture strains and field specimens from the same area, it
706 can be concluded that the observations made by Fukuyo (1981) were perfectly accurate and
707 morphological features clearly separate this species from all other known species. In addition, this
708 study also proves unambiguously that the species found in French Polynesia (*O. lenticularis*) is
709 genetically and morphologically distinct from that found in the Gulf of Thailand, especially at the
710 TF site (Tawong et al., 2014), which corresponds to the type locality of *O. siamensis*. Hence the
711 taxonomic ambiguity with *O. siamensis* should no longer persist and the absence of type for *O.*
712 *lenticularis* can be easily solved by the designation of a lectotype from the original illustrations by
713 Fukuyo (1981). The line drawing of the epitheca (Fig. 52) provides an unambiguous description of
714 the major characters, including the presence of two types of pores, which appears as the most
715 distinctive feature constant in all specimens studied from French Polynesia.

716 *Ostreopsis lenticularis* Y. Fukuyo

717 LECTOTYPE (designated here): Fig. 52 in Fukuyo (1981) Bulletin of the Japanese Society of
718 Scientific Fisheries, 47(8): p. 978.

719 5. Conclusions

720 The present re-investigation of *O. lenticularis* in French Polynesia showed that this species is
721 present in all the four archipelagos investigated, including Tahiti island and Gambier Archipelago,
722 which confirms the report by Fukuyo (1981) in the original description. The morphological features
723 observed in this study were all in perfect agreement with the original description, and the presence
724 of two kinds of thecal pores on the theca of *O. lenticularis* was seen in all specimens from cultures
725 and field samples studied. Hence this character appears as reliable taxonomic feature which can
726 distinguish *O. lenticularis* from other large-species such as *O. siamensis*, *O. labens* and *O. marina*.
727 Consequently, misidentifications of *O. lenticularis* were probably a consequence of mistaken
728 interpretations of this feature by some authors but all data appear to be congruent. From a genetic

729 point of view, the presence of a unique genotype in all the sites studied allows to associate
730 unambiguously the species name with molecular data, which was not previously possible in absence
731 of information from the type locality. Hence, the present paper provides reference sequences for
732 further molecular identifications of *O. lenticularis*. Regarding the toxicity of this species, all the
733 analyses conducted in the study showed that no toxic effect was observed using CBA-N2a assay,
734 and no PITX-like compounds could be detected from LC-MS/MS analyses, which is congruent with
735 previous data obtained by Sato et al. (2011) and Suzuki et al. (2012). Consequently, the previous
736 reports of toxicity by this species need to be re-evaluated. In particular, the toxic strains should be
737 characterized by molecular methods in order to ensure their correct identification since data in the
738 literature are confused and no unambiguous evidence of a toxicity by *O. lenticularis* has been
739 provided yet.

740

741 **Authors contributions**

742 NC and MC designed and supervised the study, drafted the paper and coordinated its revisions.
743 Moreover, MC also coordinated and contributed to the field samplings while NC also performed the
744 microscopy observations and phylogenetic analyses. GB conducted the molecular analysis and
745 sequencing. **AD contributed to editing the paper.** KH and AU contributed to the field samplings,
746 and to establishing and maintaining *Ostreopsis* clonal cultures. **JV contributed to the CBA-N2a**
747 **analysis, while HTD contributed to the CBA-N2a analysis, and to drafting and editing the**
748 **paper. CG contributed to the field samplings and to editing the paper. MR contributed to the**
749 **design of the study and to editing the paper. FH, DR and ZA developed the three**
750 **LC-(UV)-MS/MS methods and participated to the writing of the manuscript. FH also**
751 **performed extraction and chemical analyses.**

752

753 Acknowledgements

754 Tiriana Tchong and Tanguy Sergent are gratefully acknowledged for their technical assistance in
755 the extraction steps and molecular analysis, respectively. NC wish to express his deep gratitude to
756 Y. Fukuyo for sharing information on the original material from French Polynesia, and to J.
757 McNeill for kind advice on the way of dealing typification of *O. lenticularis*. This work is part of
758 the TATOO project and was supported by funds from the Délégation à la Recherche de Polynésie
759 Française (DREC-Pf). The Regional Council of Brittany, the General Council of Finistère, the
760 urban community of Concarneau Cornouaille Agglomération and the European Regional
761 Development Fund (ERDF) are also acknowledged for the funding of the Sigma 300 FE-SEM of
762 the Concarneau Marine Biology Station.

763 **References**

- 764 Accoroni, S., Romagnoli, T., Penna, A., Capellacci, S., Ciminiello, P., Dell'Aversano, C.,
 765 Tartaglione, L., Abboud-Abi Saab, M., Giussani, V., Asnagli, V., Chiantore, M., Totti, C.,
 766 2016. *Ostreopsis fattorussoi* sp. nov. (Dinophyceae), a new benthic toxic *Ostreopsis* species
 767 from the eastern Mediterranean Sea. *J. Phycol.* 52, 1064–1084.
 768 <https://doi.org/10.1111/jpy.12464>
- 769 Accoroni, S., Totti, C., 2016. The toxic benthic dinoflagellates of the genus *Ostreopsis* in temperate
 770 areas: a review. *Adv. Oceanogr. Limnol.* 7. <https://doi.org/10.4081/aiol.2016.5591>
- 771 Akselman, R., Fraga, S., 2018. other Gonyaulacales. In: IOC-UNESCO Taxon. Ref. List Harmful
 772 Micro Algae Available at <http://www.marinespecies.org/hab> (accessed 12.12.18).
- 773 Amzil, Z., Sibat, M., Chomérat, N., Gossel, H., Marco-Miralles, F., Lemée, R., Nézan, E., Séchet,
 774 V., 2012. Ovatoxin-a and Palytoxin Accumulation in seafood in relation to *Ostreopsis* cf.
 775 *ovata* blooms on the French Mediterranean coast. *Mar. Drugs* 10, 477–496.
- 776 Ariyawansa, H.A., Hawksworth, D.L., Hyde, K.D., Jones, E.B.G., Maharachchikumbura, S.S.N.,
 777 Manamgoda, D.S., Thambugala, K.M., Udayanga, D., Camporesi, E., Daranagama, A.,
 778 Jayawardena, R., Liu, J.-K., McKenzie, E.H.C., Phookamsak, R., Senanayake, I.C., Shivas,
 779 R.G., Tian, Q., Xu, J.-C., 2014. Epitypification and neotypification: guidelines with
 780 appropriate and inappropriate examples. *Fungal Divers.* 69, 57–91.
 781 <https://doi.org/10.1007/s13225-014-0315-4>
- 782 Bagnis, R., Bennett, J., Prieur, C., Legrand, A.-M., 1985. The dynamics of three toxic benthic
 783 dinoflagellates and the toxicity of ciguateric surgeonfish in French Polynesia, in: Anderson,
 784 D.M., White, A.W., Baden, D.G. (Eds.), *Toxic Dinoflagellates. Proceedings of the Third*
 785 *International Conference on Toxic Dinoflagellates. Presented at the Third International*
 786 *Conference on Toxic Dinoflagellates*, Elsevier, New York, St. Andrews, New Brunswick,
 787 Canada, pp. 177–182.

- 788 Ballantine, D., L., Bardales, A.T., Tosteson, T.R., Dupont-Durst, H., 1985. Seasonal abundance of
789 *Gambierdiscus toxicus* and *Ostreopsis* sp. in coastal waters of Southwest Puerto Rico, in:
790 Gabrié, C., Salvat, B. (Eds.). Proceedings of the Fifth International Coral Reef Congress,
791 MNHN-EPHE, pp. 417–422.
- 792 Ballantine, D., L., Tosteson, T.R., Bardales, A.T., 1988. Population dynamics and toxicity of
793 natural populations of benthic dinoflagellates in southwestern Puerto Rico. *J. Exp. Mar.*
794 *Biol. Ecol.* 119, 201–212.
- 795 Berdalet, E., Chinain, M., Fraga, S., Lemée, R., Litaker, W., Penna, A., Usup, G., Vila, M.,
796 Zingone, A., 2017. Harmful Algal Blooms in Benthic Systems: Recent Progress and Future
797 Research. *Oceanography* 30, 36–45. <https://doi.org/10.5670/oceanog.2017.108>
- 798 Brissard, C., Herrenknecht, C., Séchet, V., Hervé, F., Pisapia, F., Harcouet, J., Lemée, R.,
799 Chomérat, N., Hess, P., Amzil, Z., 2014. Complex toxin profile of French Mediterranean
800 *Ostreopsis cf. ovata* strains, seafood accumulation and ovatoxins prepurification. *Mar.*
801 *Drugs* 12, 2851–2876.
- 802 Brissard, C., Hervé, F., Sibat, M., Séchet, V., Hess, P., Amzil, Z., Herrenknecht, C., 2015.
803 Characterization of ovatoxin-h, a new ovatoxin analog, and evaluation of chromatographic
804 columns for ovatoxin analysis and purification. *J. Chromatogr. A* 1388, 87–101.
805 <https://doi.org/10.1016/j.chroma.2015.02.015>
- 806 Carlson, R.D., 1984. The distribution, periodicity, and culture of benthic/epiphytic dinoflagellates in
807 a ciguatera endemic region of the Caribbean (PhD thesis). Southern Illinois University,
808 Carbondale.
- 809 Carlson, R.D., Tindall, D.R., 1985. Distribution and periodicity of toxic dinoflagellates in the
810 Virgin Islands, in: Anderson, D.M., White, A.W., Baden, D.G. (Eds.), *Toxic*
811 *Dinoflagellates*. Proceedings of the Third International Conference on Toxic

- 812 Dinoflagellates. Presented at the International Conference on Toxic Dinoflagellates,
813 Elsevier, New York, St. Andrews, New Brunswick, Canada, pp. 171–176.
- 814 Carnicer, O., Tunin-Ley, A., Andree, K., Turquet, J., Diogène, J., Fernández-Tejedor, M., 2015.
815 Contribution to the genus *Ostreopsis* in Reunion Island (Indian Ocean): molecular,
816 morphologic and toxicity characterization. *Cryptogam. Algal.* 36, 101–119.
- 817 Castresana, J., 2000. Selection of conserved blocks from multiple alignments for their use in
818 phylogenetic analysis. *Mol. Biol. Evol.* 17, 540–552.
- 819 Chang, F.H., Shimizu, Y., Hay, B., Stewart, R., Mackay, G., Tasker, R., 2000. Three recently
820 recorded *Ostreopsis* spp. (Dinophyceae) in the New Zealand: temporal and regional
821 distribution in the upper North Island from 1995 to 1997. *N. Z. J. Mar. Freshw. Res.* 34,
822 29–39.
- 823 Chinain, M., Darius, H.T., Ung, A., Fouc, M.T., Revel, T., Cruchet, P., Pauillac, S., Laurent, D.,
824 2010. Ciguatera risk management in French Polynesia: The case study of Raivavae Island
825 (Australes Archipelago). *Toxicon* 56, 674–690.
826 <https://doi.org/10.1016/j.toxicon.2009.05.032>
- 827 Chinain, M., Faust, M.A., Pauillac, S., 1999. Morphology and molecular analyses of three toxic
828 species of *Gambierdiscus* (Dinophyceae): *G. pacificus*, sp. nov., *G. australes*, sp. nov., and
829 *G. polynesiensis*, sp. nov. *J. Phycol.* 35, 1282–1296.
- 830 Chomérat, N., Couté, A., 2008. *Protoperidinium bolmonense* sp. nov. (Peridinales, Dinophyceae),
831 a small dinoflagellate from a brackish hypereutrophic lagoon (South of France). *Phycologia*
832 47, 392–403.
- 833 Chomérat, N., Mahana iti Gatti, C., Nézan, E., Chinain, M., 2017. Studies on the benthic genus
834 *Sinophysia* (Dinophysales, Dinophyceae) II. *S. canaliculata* from Rapa Island (French
835 Polynesia). *Phycologia* 56, 193–203.

- 836 Ciminiello, P., Dell'Aversano, C., Dello Iacovo, E., Fattorusso, E., Forino, M., Grauso, L.,
837 Tartaglione, L., Guerrini, F., Pezzolesi, L., Pistocchi, R., Vanucci, S., 2012. Isolation and
838 structure elucidation of ovatoxin-a, the major toxin produced by *Ostreopsis ovata*. J. Am.
839 Chem. Soc. 134, 1869–1875. <https://doi.org/10.1021/ja210784u>
- 840 Ciminiello, P., Dell'Aversano, C., Fattorusso, E., Forino, M., Tartaglione, L., Grillo, C.,
841 Melchiorre, N., 2008. Putative palytoxin and its new analogue, ovatoxin-a, in *Ostreopsis*
842 *ovata* collected along the ligurian coasts during the 2006 toxic outbreak. J. Am. Soc. Mass
843 Spectrom. 19, 111–120. <https://doi.org/10.1016/j.jasms.2007.11.001>
- 844 Ciminiello, P., Dell'Aversano, C., Iacovo, E.D., Fattorusso, E., Forino, M., Grauso, L., Tartaglione,
845 L., Guerrini, F., Pistocchi, R., 2010. Complex palytoxin-like profile of *Ostreopsis ovata*.
846 Identification of four new ovatoxins by high-resolution liquid chromatography/mass
847 spectrometry. Rapid Commun. Mass Spectrom. 24, 2735–2744.
848 <https://doi.org/10.1002/rcm.4696>
- 849 Darius, H.T., Roué, M., Sibat, M., Viallon, J., Gatti, C.M. iti, Vandersea, M.W., Tester, P.A.,
850 Litaker, R.W., Amzil, Z., Hess, P., Chinain, M., 2018. Toxicological investigations on the
851 sea urchin *Tripneustes gratilla* (Toxopneustidae, Echinoid) from Anaho Bay (Nuku Hiva,
852 French Polynesia): Evidence for the presence of Pacific ciguatoxins. Mar. Drugs 16, 122.
853 <https://doi.org/10.3390/md16040122>
- 854 Darriba, D., Taboada, G.L., Doallo, R., Posada, D., 2012. jModelTest 2: more models, new
855 heuristics and parallel computing. Nat. Methods 9, 772. <https://doi.org/10.1038/nmeth.2109>
- 856 del Favero, G., Sosa, S., Pelin, M., D'Orlando, E., Florio, C., Lorenzon, P., Poli, M., Tubaro, A.,
857 2012. Sanitary problems related to the presence of *Ostreopsis* spp. in the Mediterranean Sea:
858 a multidisciplinary scientific approach. Ann. Inst. Sup. San. 48, 407–414.
859 https://doi.org/10.4415/ANN_12_04_08

- 860 Delgado, G., Lechuga-Devéze, C.H., Popowski, G., Troccoli, L., Salinas, C.A., 2006. Epiphytic
861 dinoflagellates associated with ciguatera in the northwestern coast of Cuba. *Rev. Biol. Trop.*
862 54, 299–310.
- 863 Faust, M.A., 1999. Three new *Ostreopsis* species (Dinophyceae): *O. marinus* sp. nov., *O.*
864 *belizeanus* sp. nov., and *O. caribbeanus* sp. nov. *Phycologia* 38, 92–99.
- 865 Faust, M.A., 1995. Observation of sand-dwelling toxic dinoflagellates (Dinophyceae) from widely
866 differing sites, including two new species. *J. Phycol.* 31, 996–1003.
- 867 Faust, M.A., Gulledge, R.A., 2002. Identifying harmful marine dinoflagellates. *Smithson. Inst.*
868 *Contrib. U. S. Natl. Herb.* 42, 1–144.
- 869 Faust, M.A., Morton, S.L., 1995. Morphology and ecology of the marine dinoflagellate *Ostreopsis*
870 *labens* sp. nov. (Dinophyceae). *J. Phycol.* 31, 456–463.
- 871 Faust, M.A., Morton, S.L., Quod, J.-P., 1996. Further SEM study of marine dinoflagellates: the
872 genus *Ostreopsis* (Dinophyceae). *J. Phycol.* 32, 1053–1065.
- 873 Fukuyo, Y., 1981. Taxonomical study on benthic dinoflagellates collected in coral reefs. *Bull. Jpn.*
874 *Soc. Sci. Fish.* 47, 967–978.
- 875 Gárate-Lizárraga, I., González-Armas, R., Okolodkov, Y.B., 2018. Occurrence of *Ostreopsis*
876 *lenticularis* (Dinophyceae: Gonyaulacales) from the Archipiélago de Revillagigedo,
877 Mexican Pacific. *Mar. Pollut. Bull.* 128, 390–395.
878 <https://doi.org/10.1016/j.marpolbul.2018.01.020>
- 879 García-Altres, M., Tartaglione, L., Dell’Aversano, C., Carnicer, O., de la Iglesia, P., Forino, M.,
880 Diogène, J., Ciminiello, P., 2015. The novel ovatoxin-g and isobaric palytoxin (so far
881 referred to as putative palytoxin) from *Ostreopsis* cf. *ovata* (NW Mediterranean Sea):
882 structural insights by LC-high resolution MS. *Anal. Bioanal. Chem.* 407, 1191–1204.
883 <https://doi.org/10.1007/s00216-014-8338-y>

- 884 Gouy, M., Guindon, S., Gascuel, O., 2010. SeaView Version 4: A Multiplatform Graphical User
885 Interface for Sequence Alignment and Phylogenetic Tree Building. *Mol. Biol. Evol.* 27,
886 221–224. <https://doi.org/10.1093/molbev/msp259>
- 887 Guindon, S., Dufayard, J.-F., Lefort, V., Anisimova, M., Hordijk, W., Gascuel, O., 2010. New
888 algorithms and methods to estimate Maximum-Likelihood phylogenies: assessing the
889 performance of PhyML 3.0. *Syst. Biol.* 59, 307–21.
- 890 Hansen, G., Turquet, J., Quod, J.-P., Ten-Hage, L., Lugomela, C., Kyewalyanga, M., Hurbungs, M.,
891 Wawiye, P., Ogongo, B., Tunje, S., Rakotoarinjanahary, H., 2001. Potentially harmful
892 microalgae of the western Indian Ocean, Manual and guides. Intergovernmental
893 Oceanographic Commission of UNESCO.
- 894 Holmes, M.J., Lewis, R.J., Poli, M.A., Gillespie, N.C., 1991. Strain dependent production of
895 ciguatoxin precursors (gambiertoxins) by *Gambierdiscus toxicus* (Dinophyceae) in culture.
896 *Toxicon* 29, 761–775. [https://doi.org/10.1016/0041-0101\(91\)90068-3](https://doi.org/10.1016/0041-0101(91)90068-3)
- 897 Hoppenrath, M., 2017. Dinoflagellate taxonomy — a review and proposal of a revised
898 classification. *Mar. Biodivers.* 47, 381–403. <https://doi.org/10.1007/s12526-016-0471-8>
- 899 Hoppenrath, M., Murray, S., Chomérat, N., Horiguchi, T., 2014. Marine benthic dinoflagellates -
900 unveiling their worldwide biodiversity (Kleine Senckenberg-Reihe 54). E.
901 Schweizerbart'sche Verlagbuchhandlung.
- 902 Katoh, K., Standley, D.M., 2013. MAFFT multiple sequence alignment software version 7:
903 improvements in performance and usability. *Mol. Biol. Evol.* 30, 772–80.
904 <https://doi.org/10.1093/molbev/mst010>
- 905 Kumar, S., Stecher, G., Li, M., Knyaz, C., Tamura, K., 2018. MEGA X: Molecular Evolutionary
906 Genetics Analysis across Computing Platforms. *Mol. Biol. Evol.* 35, 1547–1549.
907 <https://doi.org/10.1093/molbev/msy096>

- 908 Larsen, J., Nguyen Ngoc, L., 2004. Potentially toxic microalgae of Vietnamese waters, *Opera Bot.*
909 140, 5–216.
- 910 Lassus, P., Chomérat, N., Hess, P., Nézan, E., 2016. Toxic and harmful microalgae of the world
911 ocean. UNESCO, Denmark.
- 912 Leaw, C.P., Lim, P.T., Asmat, A., Usup, G., 2001. Genetic Diversity of *Ostreopsis ovata*
913 (Dinophyceae) from Malaysia. *Mar. Biotechnol.* 3, 246–255.
914 <https://doi.org/10.1007/s101260000073>
- 915 Ledreux, A., Krys, S., Bernard, C., 2009. Suitability of the Neuro-2a cell line for the detection of
916 palytoxin and analogues (neurotoxic phycotoxins). *Toxicon* 53, 300–308.
917 <https://doi.org/10.1016/j.toxicon.2008.12.005>
- 918 Lenoir, S., Ten-Hage, L., Turquet, J., Quod, J.-P., Bernard, C., Hennion, M.-C., 2004. First
919 evidence of palytoxin analogues from an *Ostreopsis mascarenensis* (Dinophyceae) benthic
920 bloom in southwestern Indian Ocean. *J. Phycol.* 40, 1042–1051.
- 921 Marchan-Álvarez, J., Valerio-González, L., Troccoli-Ghinaglia, L., Monroy, F.L., 2017.
922 Dinoflagelados bentónicos nocivos, asociados con el sedimento arenoso en dos playas de la
923 isla de Margarita, Venezuela. *Rev. Biodivers. Neotropical* 7, 156–168.
- 924 Mercado, J.A., Vieira, M., Escalona de Motta, G., Tosteson, T.R., Gonzalez, I., Silva, W., 1994. An
925 extraction procedure modification changes the toxicity, chromatographic profile and
926 pharmacologic action of *Ostreopsis lenticularis* extracts. *Toxicon* 32, 256.
- 927 Mercado, J.A., Viera, M., Tosteson, T.R., González, I., Silva, W., Escalona de Motta, G., 1995.
928 Differences in the toxicity and biological activity of *Ostreopsis lenticularis* observed using
929 different extraction procedures, in: Lassus, P., Arzul, G., Erard-Le Denn, E., Gentien, P.,
930 Marcaillou-le Baut, C. (Eds.), *Harmful Marine Algal Blooms. Proceedings of the Sixth*
931 *International Conference on Toxic Marine Phytoplankton, October 1993, Nantes, France,*
932 *Lavoisier, Intercept Ltd, Nantes.*

- 933 Meunier, F.A., Mercado, J.A., Molgó, J., Tosteson, T.R., Escalona de Motta, G., 1997. Selective
934 depolarization of the muscle membrane in frog nerve-muscle preparations by a
935 chromatographically purified extract of the dinoflagellate *Ostreopsis lenticularis*. Br. J.
936 Pharmacol. 121, 1224–1230. <https://doi.org/10.1038/sj.bjp.0701256>
- 937 Moore, R.E., Scheuer, P.J., 1971. Palytoxin: a new marine toxin from a Coelenterate. Science 172,
938 495–498.
- 939 Nézan, E., Siano, R., Boulben, S., Six, C., Bilien, G., Chèze, K., Duval, A., Le Panse, S., Quéré, J.,
940 Chomérat, N., 2014. Genetic diversity of the harmful family Kareniaceae (Gymnodiniales,
941 Dinophyceae) in France, with the description of *Karlodinium gentienii* sp. nov.: A new
942 potentially toxic dinoflagellate. Harmful Algae 40, 75–91.
943 <https://doi.org/10.1016/j.hal.2014.10.006>
- 944 Norris, D.R., Bomber, J.W., Balech, E., 1985. Benthic dinoflagellates associated with ciguatera
945 from the Florida Keys. I. *Ostreopsis heptagona* sp. nov., in: Anderson, D.M., White, A.W.,
946 Baden, D.G. (Eds.), Toxic Dinoflagellates. Elsevier Science publ. Co., New York, pp.
947 39–44.
- 948 Parsons, M.L., Aligizaki, K., Dechraoui Bottein, M.-Y., Fraga, S., Morton, S.L., Penna, A., Rhodes,
949 L., 2012. *Gambierdiscus* and *Ostreopsis*: Reassessment of the state of knowledge of their
950 taxonomy, geography, ecophysiology, and toxicology. Harmful Algae 14, 107–129.
- 951 Pawlowicz, R., Darius, H.T., Cruchet, P., Rossi, F., Caillaud, A., Laurent, D., Chinain, M., 2013.
952 Evaluation of seafood toxicity in the Australes archipelago (French Polynesia) using the
953 neuroblastoma cell-based assay. Food Addit. Contam. Part A 30, 567–586.
954 <https://doi.org/10.1080/19440049.2012.755644>
- 955 Penna, A., Fraga, S., Battocchi, C., Casabianca, S., Giacobbe, M.G., Riobó, P., Vernesi, C., 2010. A
956 phylogeographical study of the toxic benthic dinoflagellate genus *Ostreopsis* Schmidt. J.
957 Biogeogr. 37, 830–841.

- 958 Penna, A., Fraga, S., Battocchi, C., Casabianca, S., Perini, F., Capellacci, S., Casabianca, A., Riobó,
959 P., Giacobbe, M.G., Totti, C., Accoroni, S., Vila, M., Reñé, A., Scardi, M., Aligizaki, K.,
960 Nguyen-Ngoc, L., Vernesi, C., 2012. Genetic diversity of the genus *Ostreopsis* Schmidt:
961 Phylogeographical considerations and molecular methodology applications for field
962 detection in the Mediterranean Sea. *Cryptogam. Algol.* 33, 153–163.
963 <https://doi.org/10.7872/crya.v33.iss2.2011.153>
- 964 Penna, A., Vila, M., Fraga, S., Giacobbe, M.G., Andreoni, F., Riobó, P., Vernesi, C., 2005.
965 Characterization of *Ostreopsis* and *Coolia* (Dinophyceae) isolates in the western
966 mediterranean sea based on morphology, toxicity and internal transcribed spacer 5.8S rDNA
967 sequences. *J. Phycol.* 41, 212–225.
- 968 Pérez-Guzmán, L., Pérez-Matos, A.E., Rosado, W., Tosteson, T.R., Govind, N.S., 2008. Bacteria
969 associated with toxic clonal cultures of the dinoflagellate *Ostreopsis lenticularis*. *Mar.*
970 *Biotechnol.* 10, 492–496. <https://doi.org/10.1007/s10126-008-9088-7>
- 971 Quod, J.-P., 1994. *Ostreopsis mascarenensis* sp. nov. (Dinophyceae), dinoflagellé toxique associé à
972 la ciguatera dans l’océan Indien. *Cryptogam. Algol.* 15, 243–251.
- 973 Rasband, W.S., 1997. ImageJ. National Institutes of Health, Bethesda, Maryland.
- 974 Rhodes, L., Adamson, J., Suzuki, T., Briggs, L., Garthwaite, I., 2000. Toxic marine epiphytic
975 dinoflagellates, *Ostreopsis siamensis* and *Coolia monotis* (Dinophyceae), in New Zealand.
976 *N. Z. J. Mar. Freshw. Res.* 34, 371–383.
- 977 Ronquist, F., Huelsenbeck, J.P., 2003. MrBayes 3: Bayesian phylogenetic inference under mixed
978 models. *Bioinformatics* 19, 1572–1574.
- 979 Rossi, R., Castellano, V., Scalco, E., Serpe, L., Zingone, A., Soprano, V., 2010. New palytoxin-like
980 molecules in Mediterranean *Ostreopsis* cf. *ovata* (dinoflagellates) and in *Palythoa*
981 *tuberculosa* detected by liquid chromatography-electrospray ionization time-of-flight mass
982 spectrometry. *Toxicon* 56, 1381–1387. <https://doi.org/10.1016/j.toxicon.2010.08.003>

- 983 Sanchez, R., Serra, F., Tarraga, J., Medina, I., Carbonell, J., Pulido, L., de Maria, A.,
984 Capella-Gutierrez, S., Huerta-Cepas, J., Gabaldon, T., Dopazo, J., Dopazo, H., 2011.
985 Phylemon 2.0: a suite of web-tools for molecular evolution, phylogenetics, phylogenomics
986 and hypotheses testing. *Nucleic Acids Res.* 39, W470–W474.
987 <https://doi.org/10.1093/nar/gkr408>
- 988 Sato, S., Nishimura, T., Uehara, K., Sakanari, H., Tawong, W., Hariganeya, N., Smith, K., Rhodes,
989 L., Yasumoto, T., Taira, Y., Suda, S., Yamaguchi, H., Adachi, M., 2011. Phylogeography of
990 *Ostreopsis* along west Pacific coast, with special reference to a novel clade from Japan. *Plos*
991 *One* 6, e27983. <https://doi.org/10.1371/journal.pone.0027983>
- 992 Schmidt, J., 1901. Preliminary report of the botanical results of the Danish expedition to Siam
993 (1899-1900). Part IV, Peridiniales. *Bot. Tidsskr.* 24, 212–221.
- 994 Suzuki, T., Watanabe, R., Uchida, H., Matsushima, R., Nagai, H., Yasumoto, T., Yoshimatsu, T.,
995 Sato, S., Adachi, M., 2012. LC-MS/MS analysis of novel ovatoxin isomers in several
996 *Ostreopsis* strains collected in Japan. *Harmful Algae* 20, 81–91.
997 <https://doi.org/10.1016/j.hal.2012.08.002>
- 998 Tartaglione, L., Dello Iacovo, E., Mazzeo, A., Casabianca, S., Ciminiello, P., Penna, A.,
999 Dell’Aversano, C., 2017. Variability in toxin profiles of the Mediterranean *Ostreopsis* cf.
1000 *ovata* and in structural features of the produced ovatoxins. *Environ. Sci. Technol.* 51,
1001 13920–13928. <https://doi.org/10.1021/acs.est.7b03827>
- 1002 Tartaglione, L., Mazzeo, A., Dell’Aversano, C., Forino, M., Giussani, V., Capellacci, S., Penna, A.,
1003 Asnaghi, V., Faimali, M., Chiantore, M., Yasumoto, T., Ciminiello, P., 2016. Chemical,
1004 molecular, and eco-toxicological investigation of *Ostreopsis* sp. from Cyprus Island:
1005 structural insights into four new ovatoxins by LC-HRMS/MS. *Anal. Bioanal. Chem.* 408,
1006 915–932. <https://doi.org/10.1007/s00216-015-9183-3>

- 1007 Tawong, W., Nishimura, T., Sakanari, H., Sato, S., Yamaguchi, H., Adachi, M., 2014. Distribution
1008 and molecular phylogeny of the dinoflagellate genus *Ostreopsis* in Thailand. *Harmful Algae*
1009 37, 160–171. <https://doi.org/10.1016/j.hal.2014.06.003>
- 1010 Terajima, T., Uchida, H., Abe, N., Yasumoto, T., 2018. Structure elucidation of ostreocin-A and
1011 ostreocin-E1, novel palytoxin analogs produced by the dinoflagellate *Ostreopsis siamensis* ,
1012 using LC/Q-TOF MS. *Biosci. Biotechnol. Biochem.* 1–10.
1013 <https://doi.org/10.1080/09168451.2018.1550356>
- 1014 Tester, P.A., Kibler, S.R., Holland, W.C., Usup, G., Vandersea, M.W., Leaw, C.P., Teen, L.P.,
1015 Larsen, J., Mohammad-Noor, N., Faust, M.A., Litaker, R.W., 2014. Sampling harmful
1016 benthic dinoflagellates: Comparison of artificial and natural substrate methods. *Harmful*
1017 *Algae* 39, 8–25. <https://doi.org/10.1016/j.hal.2014.06.009>
- 1018 Tichadou, L., Glaizal, M., Armengaud, A., Grosseil, H., Lemée, R., Kantin, R., Lasalle, J.-L.,
1019 Drouet, G., Rambaud, L., Malfait, P., de Haro, L., 2010. Health impact of unicellular algae
1020 of the *Ostreopsis* genus blooms in the Mediterranean Sea: experience of the French
1021 Mediterranean coast surveillance network from 2006 to 2009. *Clin. Toxicol.* 48, 839–844.
1022 <https://doi.org/10.3109/15563650.2010.513687>
- 1023 Tindall, D.R., Miller, D.M., Tindall, P.M., 1990. Toxicity of *Ostreopsis lenticularis* from the
1024 British and United States Virgin Islands, in: Granéli, E., Sundström, B., Edler, L., Anderson,
1025 D.M. (Eds.), *Toxic Marine Phytoplankton. Proceedings of the Fourth International*
1026 *Conference on Toxic Marine Phytoplankton.* Elsevier, Lund, Sweden, pp. 424–429.
- 1027 Tosteson, T.R., Ballantine, D., L., Tosteson, C.G., Bardales, A.T., Durst, H.D., Higerd, T.B., 1986.
1028 Comparative toxicity of *Gambierdiscus toxicus*, *Ostreopsis* cf. *lenticularis*, and associated
1029 microflora. *Mar. Fish. Rev.* 48, 57–59.

- 1030 Tosteson, T.R., Ballantine, D.L., Tosteson, C.G., Hensley, V., Bardales, A.T., 1989. Associated
1031 bacterial flora, growth, and toxicity of cultured benthic dinoflagellates *Ostreopsis*
1032 *lenticularis* and *Gambierdiscus toxicus*. Appl. Environ. Microbiol. 55, 5.
- 1033 Turland, N.J., Wiersema, J.H., Barrie, F.R., Greuter, W., Hawksworth, D.L., Herendeen, P.S.,
1034 Knapp, S., Kusber, W.-H., Li, D.-Z., Marhold, K., May, T.W., McNeill, J., Monro, A.M.,
1035 Prado, J., Price, M.J., Smith, G.F. (Eds.), 2018. International Code of Nomenclature for
1036 algae, fungi, and plants (Shenzhen Code) adopted by the Nineteenth International Botanical
1037 Congress Shenzhen, China, July 2017, Regnum Vegetabile. Koeltz Botanical Books,
1038 Glasshütten.
- 1039 Uchida, H., Taira, Y., Yasumoto, T., 2013. Structural elucidation of palytoxin analogs produced by
1040 the dinoflagellate *Ostreopsis ovata* IK2 strain by complementary use of positive and
1041 negative ion liquid chromatography/quadrupole time-of-flight mass spectrometry: Structural
1042 elucidation of ovatoxin-a, -d, -e IK2 by LC/QTOFMS. Rapid Commun. Mass Spectrom. 27,
1043 1999–2008. <https://doi.org/10.1002/rcm.6657>
- 1044 Ukena, T., Satake, M., Usami, M., Oshima, Y., Naoki, H., Fujita, T., Kan, Y., Yasumoto, T., 2001.
1045 Structure elucidation of Ostreocin D, a palytoxin analog isolated from the dinoflagellate
1046 *Ostreopsis siamensis*. Biosci. Biotechnol. Biochem. 65, 2585–2588.
1047 <https://doi.org/10.1271/bbb.65.2585>
- 1048 Usami, M., Satake, M., Ishida, S., Inoue, A., Kan, Y., Yasumoto, T., 1995. Palytoxin analogs from
1049 the dinoflagellate *Ostreopsis siamensis*. J. Am. Chem. Soc. 117, 5389–5390.
- 1050 Verma, A., Hoppenrath, M., Dorantes-Aranda, J.J., Harwood, D.T., Murray, S.A., 2016. Molecular
1051 and phylogenetic characterization of *Ostreopsis* (Dinophyceae) and the description of a new
1052 species, *Ostreopsis rhodesae* sp. nov., from a subtropical Australian lagoon. Harmful Algae
1053 60, 116–130. <https://doi.org/10.1016/j.hal.2016.11.004>

- 1054 Zhang, H., Lu, S., Li, Y., Cen, J., Wang, H., Li, Q., Nie, X., 2018. Morphology and molecular
1055 phylogeny of *Ostreopsis* cf. *ovata* and *O. lenticularis* (Dinophyceae) from Hainan Island,
1056 South China Sea: *Ostreopsis* spp. from Hainan Island. *Phycol. Res.* 66, 3–14.
1057 <https://doi.org/10.1111/pre.12192>
1058

1059 **Figure legends**

1060 **Fig. 1.** Map of French Polynesia (South Pacific Ocean), showing the location of the different
1061 archipelagos. The islands from where samples of *Ostreopsis lenticularis* were collected are
1062 encircled by thick lines.

1063

1064 **Fig. 2.** Light and epifluorescence micrographs of cells from strain THT16–4 from Tahiti Island
1065 (Society Archipelago). (A) Live specimen; (B) epifluorescence image showing the nucleus stained
1066 by SYBR green. Scale bars: 10 μm .

1067

1068 **Fig. 3.** Epifluorescence micrographs of different strains and field specimens of *Ostreopsis*
1069 *lenticularis*. (A–C) strain THT16–4 from Tahiti Island (Society Archipelago): (A) apical view; (B)
1070 antapical view; (C) detail of the apical pore and adjacent plates, note the presence of two kind of
1071 thecal pores (some smaller pores shown by arrowheads). (D–G) strain MGR17–1 from Mangareva
1072 Island (Gambier Archipelago): (D) apical view; (E) antapical view; (F) detail of the apical pore and
1073 adjacent plate; (G) detail of the thecal surface with two kinds of thecal pores. (H–K) strain
1074 RVV-RF8 from Raivavae Island (Australes Archipelago): (H) apical view; (I) antapical view; (J)
1075 detail of the apical pore and adjacent plates; (K) detail of the thecal surface with two kinds of thecal
1076 pores. (L–M) strain TIO6 from Nuku Hiva Island (Marquesas Archipelago): (L) apical view; (M)
1077 antapical view. (N–O) field specimens from Anaho Bay (Nuku Hiva Island): (N) apical view; (O)
1078 antapical view. Scale bars: 20 μm in A, B, D, E, H, I, L– O, 10 μm in F, J, 5 μm in C, K, and 2 μm
1079 in G.

1080

1081 **Fig. 4.** Scanning electron micrographs of cells from strain THT16–4 (Tahiti Island, Society
1082 Archipelago). (A) apical view; (B) antapical view; (C) ventral view; (D) left lateral view showing
1083 the straight cingulum and apical pore plate (Po). Scale bars: 10 μm .

1084

1085 **Fig. 5.** Scanning electron micrographs of cells from strain THT16–4 (Tahiti Island, Society
1086 Archipelago). (A) detail of apical plate series and apical pore; (B) detail of the Po plate and apical
1087 pore composed by a slit and 2 rows of pores; (C) ventral view of the sulcus, note the presence of a
1088 partially visible sulcal plate (arrowhead), a list on the Sda plate (asterisk) and the flagellar pore (fp);
1089 (D) detail of the thecal pores of two sizes, note that the internal structure is visible within larger
1090 pores. Scale bars: 2 μm in A, B and C, and 1 μm in D.

1091

1092 **Fig. 6.** Scanning electron micrographs of field specimens from Anaho Bay, Nuku Hiva Island
1093 (Marquesas Archipelago). (A) apical view; (B) antapical view; (C) ventral view; (D)
1094 ventro-antapical view showing the cell flattening; (E) detail of apical plates and apical pore (Po);
1095 (F) detail of sulcal plates, note that a plate is only partially visible (arrowhead) and the flagellar pore
1096 (fp); (G) detail of the surface of the theca with two kinds of pores. Scale bars: 10 μm in A–D, 2 μm
1097 in E, and 1 μm in F–G.

1098

1099 **Fig. 7.** Maximum Likelihood phylogenetic tree inferred from LSU D8–D10 sequences of various
1100 *Ostreopsis* strains. French Polynesian strains are indicated by bold face and a gray background.
1101 *Coolia* sp. is used as an outgroup. Black vertical bars show distinct *Ostreopsis* clade. For *O.* cf.
1102 *ovata*, three subclades are shown: Med/Pac for Mediterranean and Pacific subclade; SCS for the
1103 South China Sea subclade and Thai for the Thailand subclade. For *O. lenticularis*, the vertical gray
1104 bars show the geographic origin of the strains. Numbers at nodes represent bootstrap support values

1105 from Maximum Likelihood (ML) and posterior probabilities from Bayesian Inference (BI).

1106 Bootstraps values below 55 and posterior probabilities below 0.70 are not shown. Roman numerals
1107 (I-V) indicate the subclades as defined in Table 2.

1108

1109 **Fig. 8.** Maximum Likelihood phylogenetic tree inferred from ITS–5.8S rDNA sequences of various
1110 *Ostreopsis* strains. *Coolia monotis* is used as an outgroup. French Polynesian strains are indicated
1111 by bold face and a gray background. Black vertical bars show distinct *Ostreopsis* clade. For *O. cf.*
1112 *ovata*, three subclades are shown: SCS for the South China Sea subclade, Thai/Ind for the
1113 Thailand/Indonesia subclade, and Med/Atl/Pac for Mediterranean, Atlantic and Pacific subclade.
1114 For *O. lenticularis*, the vertical gray bars indicate the geographic origin of the strains. Numbers at
1115 nodes represent bootstrap support values from Maximum Likelihood (ML) and posterior
1116 probabilities from Bayesian Inference (BI). Bootstraps values below 50 and posterior probabilities
1117 below 0.70 are not shown. Roman numerals (I-VII) indicate the subclades as defined in Table 3.

1118

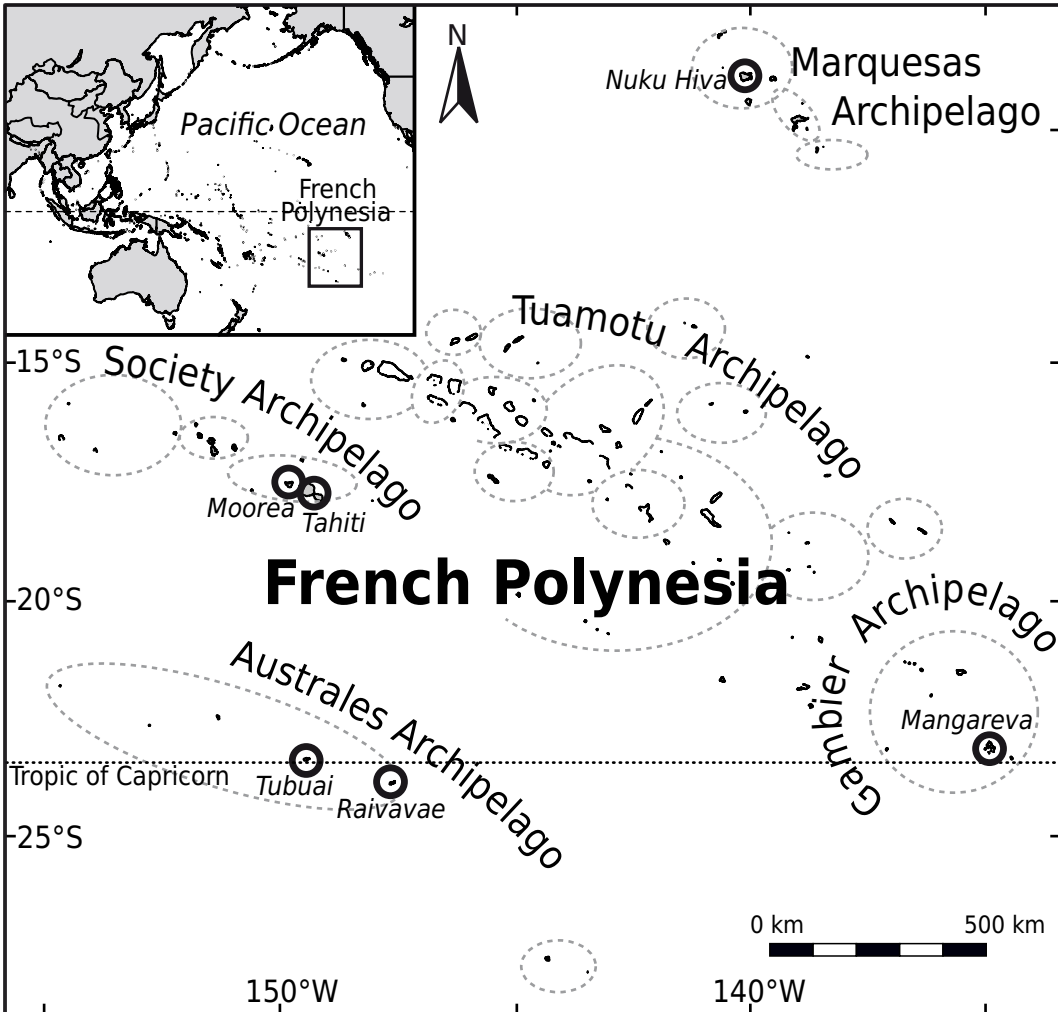
1119 **Supplementary material**

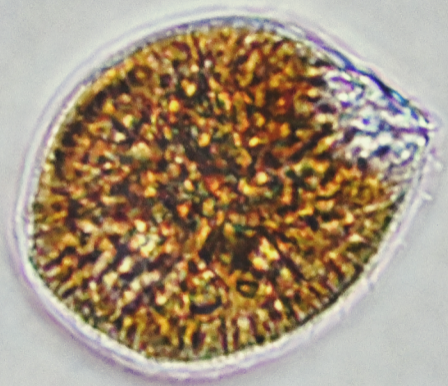
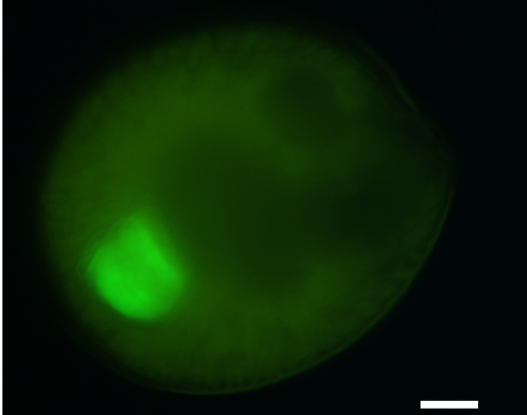
1120 **Fig. S1.** Scanning electron micrographs of cells from strains from different archipelagos. (A–C)
1121 strain RVV-RF8 (Australes Archipelago) (A) apical view; (B) antapical view; (C) detail of thecal
1122 surface; (D–F) strain MGR17–1 (Gambier Archipelago): (D) apical view; (E) antapical view; (F)
1123 detail of thecal surface; (G–I) strain TIO6 (Marquesas Archipelago): (G) apical view; (H) antapical
1124 view; (I) detail of thecal surface;. Scale bars: 10 μm in A, B, D, E, G, H, and 1 μm in C, F and I.

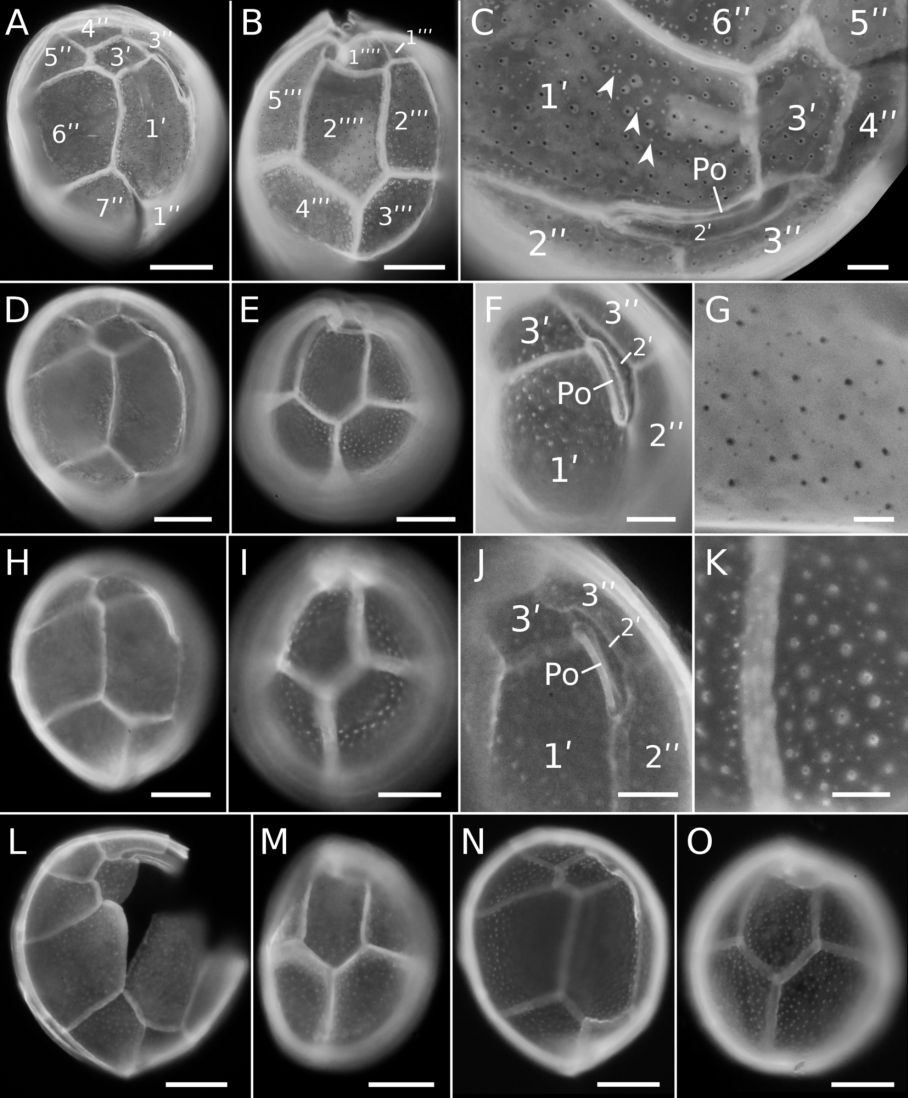
1125

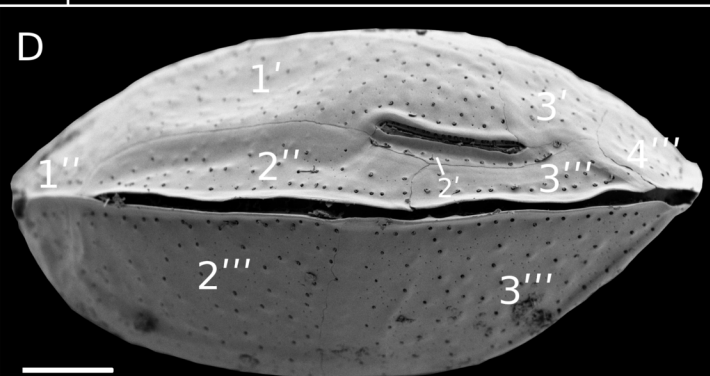
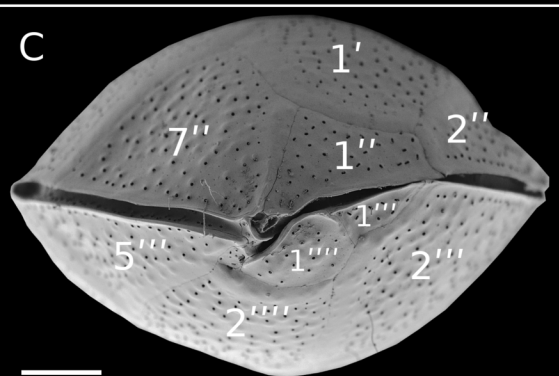
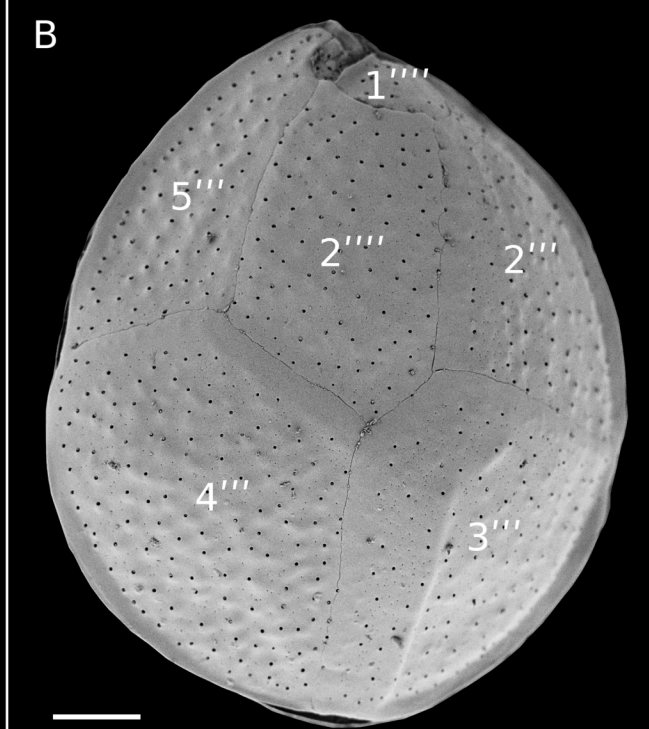
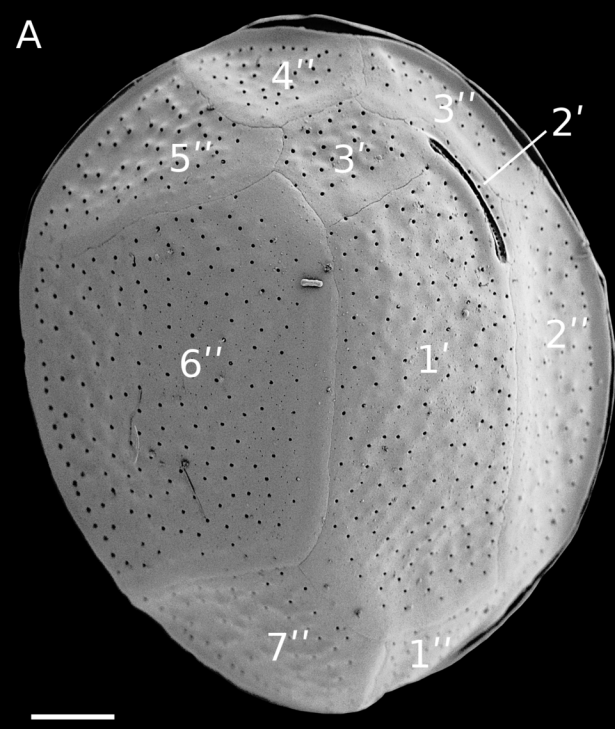
1126 **Fig. S2.** Scanning electron micrographs of cells from strain THT16–4 (Tahiti Island, Society
1127 Archipelago) showing cingular plates. (A) Detail of the sulcus and the first cingular plate C1
1128 (arrowheads points to the suture); (B) left lateral view of a cell with three cingular plates visible

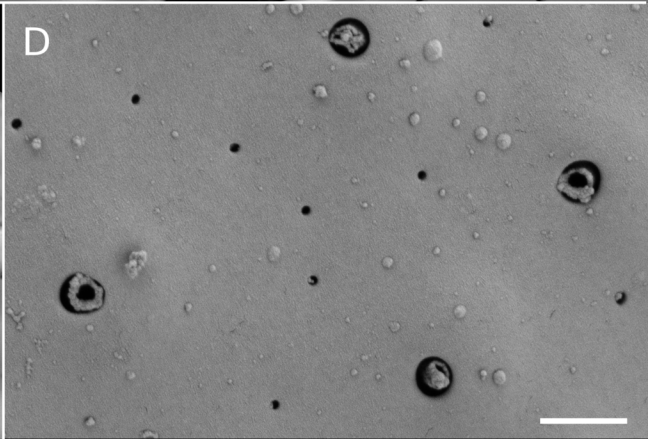
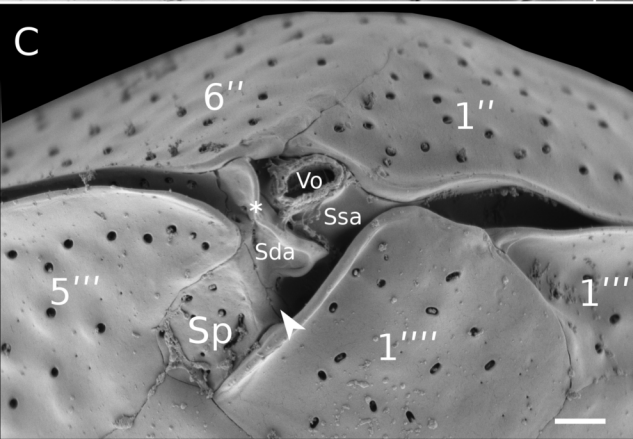
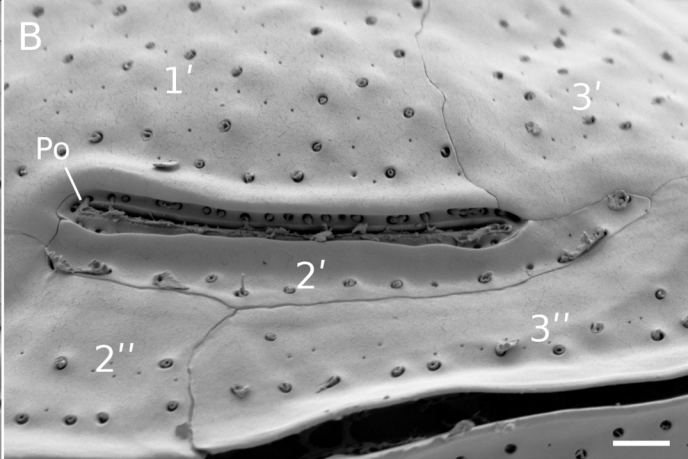
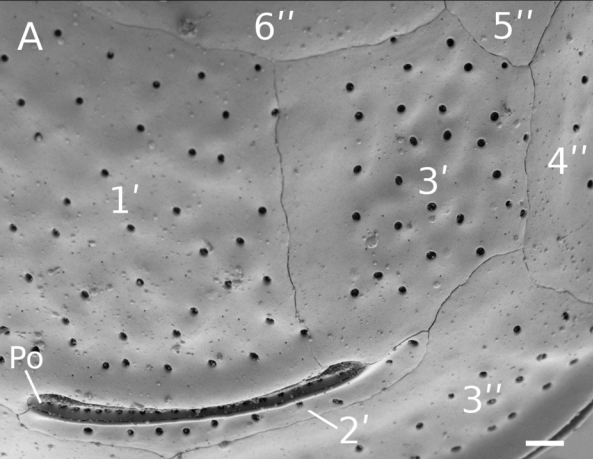
1129 (arrowheads point to the sutures); (C) Right dorsal view showing plates C3, C4 and C5 (arrowheads
1130 point to the sutures); (D) right lateral view showing plates C5 and C6 (arrowheads point to the
1131 sutures). Scale bars: 1 μm in A and 5 μm in B, C, D.

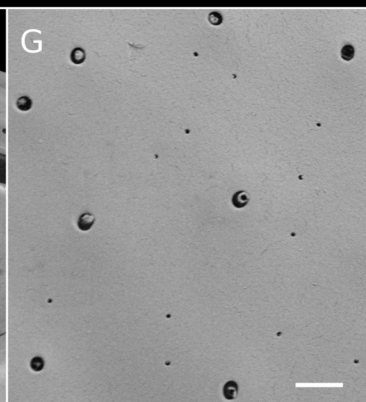
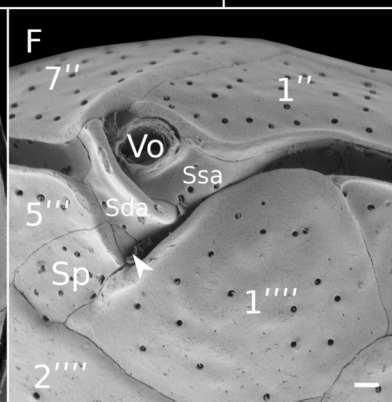
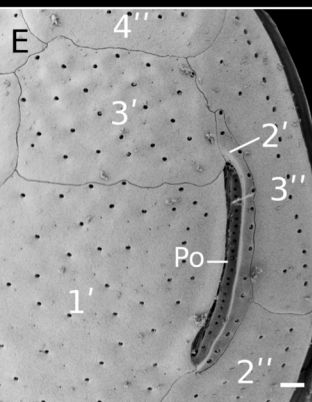
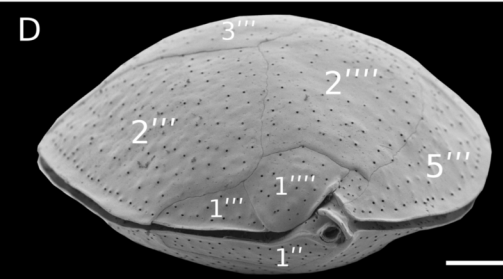
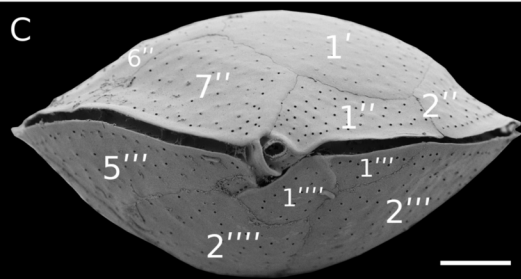
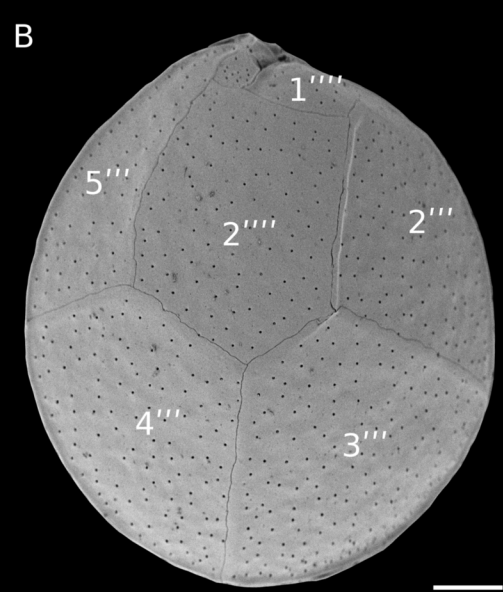
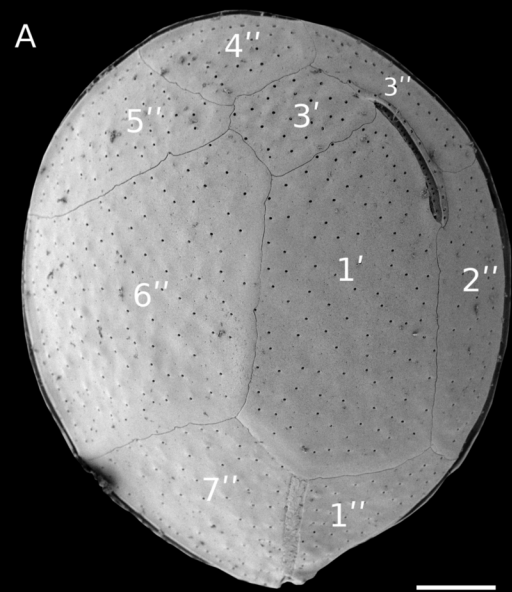


A**B**

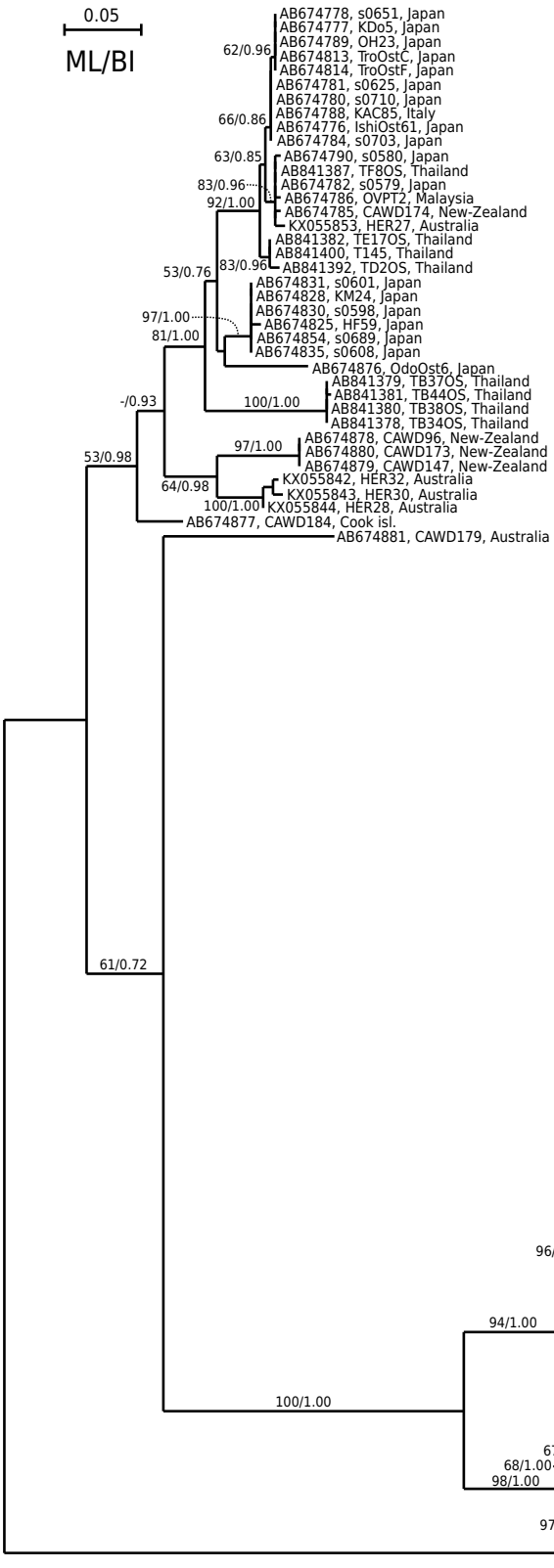








0.05
ML/BI



- MK227190, RVV-RF8, Raivavae
- MK227194, Tub8, Tubuai
- MK227195, Tub9, Tubuai
- MK227196, Tub10, Tubuai
- MK227197, Tub11, Tubuai
- MK227198, Tub12, Tubuai
- MK227199, Tub14, Tubuai
- MK227200, Tub15, Tubuai
- MK227201, Tub22, Tubuai
- MK227202, Tub23, tubuai
- MK227203, Tub24, Tubuai
- MK227204, Tub25, Tubuai
- MK227205, Tub26, Tubuai
- MK227206, Tub27, Tubuai
- MK227207, Tub28, Tubuai
- MK227208, Tub30, Tubuai
- MK227209, Tub29, Tubuai
- MK227210, Tub31, Tubuai
- MK227211, Tub32, Tubuai
- MK227191, MTR17-1, Tubuai
- MK227192, MTR17-2, Tubuai
- MK227193, MTR17-3, Tubuai
- MK227215, NH16-7, Nuku Hiva
- MK227216, ANH33, Nuku Hiva
- MK227217, ANH34, Nuku Hiva
- MK227218, TIO6, Nuku Hiva
- MK227219, TIO7, Nuku Hiva
- MK227220, TPV1, Nuku Hiva
- MK227221, TPV2, Nuku Hiva
- MK227222, TPV3, Nuku Hiva
- MK227223, TPV4, Nuku Hiva
- MK227224, TPV5, Nuku Hiva
- MK227225, TPV6, Nuku Hiva
- MK227226, TPV9, Nuku Hiva
- MK227227, IFR17-088, Nuku Hiva
- MK227228, IFR17-107, Nuku Hiva
- MK227229, IFR17-118, Nuku Hiva
- MK227186, THT16-1, Tahiti
- MK227187, THT16-2, Tahiti
- MK227188, THT16-4, Tahiti
- MK227189, VRO17-1, Tahiti
- MK227180, ATH6, Moorea
- MK227181, HPT6, Moorea
- MK227182, MRP23, Moorea
- MK227183, MRP25, Moorea
- MK227184, MRP26, Moorea
- MK227185, MD03-03, Tahiti
- MK227212, MGR17-1, Mangareva
- MK227213, MGR17-2, Mangareva
- MK227214, MGR17-3, Mangareva
- AB674888, s0577, Iriomote, Japan
- AB674889, s0578, Iriomote, Japan
- AB674885, IkeOst2, Okinawa, Japan
- AB674884, O70421-2, Shikoku, Japan
- AB674893, s0808, Shikoku, Japan
- AB674883, O70421-1, Shikoku, Japan
- AB674890, s0627, Shikoku, Japan
- AB674894, s0809, Shikoku, Japan
- AB674892, s0806, Shikoku, Japan
- AB674891, s0780, Shikoku, Japan
- AB674882, MB80828-4, Shikoku, Japan
- AB674886, MB80828-2, Shikoku, Japan
- AB674887, O70421-3, Shikoku, Japan
- AB674898, IR49, Iriomote, Japan
- AB674895, IR33, Iriomote, Japan
- AB674899, OUB, Okinawa, Japan
- AB674896, OUI, Okinawa, Japan
- AB674900, s0595, Kohama, Japan
- AB674897, s0587, Iriomote, Japan
- AB841410, TF29OS, Thailand
- AB841409, TF25OS, Thailand
- AB674901, *Coolia* sp., Japan

Med/Pac
SCS
Thai
Austral
FRENCH POLYNESIA
French Polynesia/ South Japan
I.
Marquesas
Society
Gambier
North Japan
II.
III.
IV.
V.

O. cf. ovata

Ostreopsis sp. 1

Ostreopsis sp. 2

Ostreopsis sp. 7

O. cf. siamensis

O. rhodesiae

Ostreopsis sp. 3

Ostreopsis sp. 4

O. lenticularis
(= sp. 5)

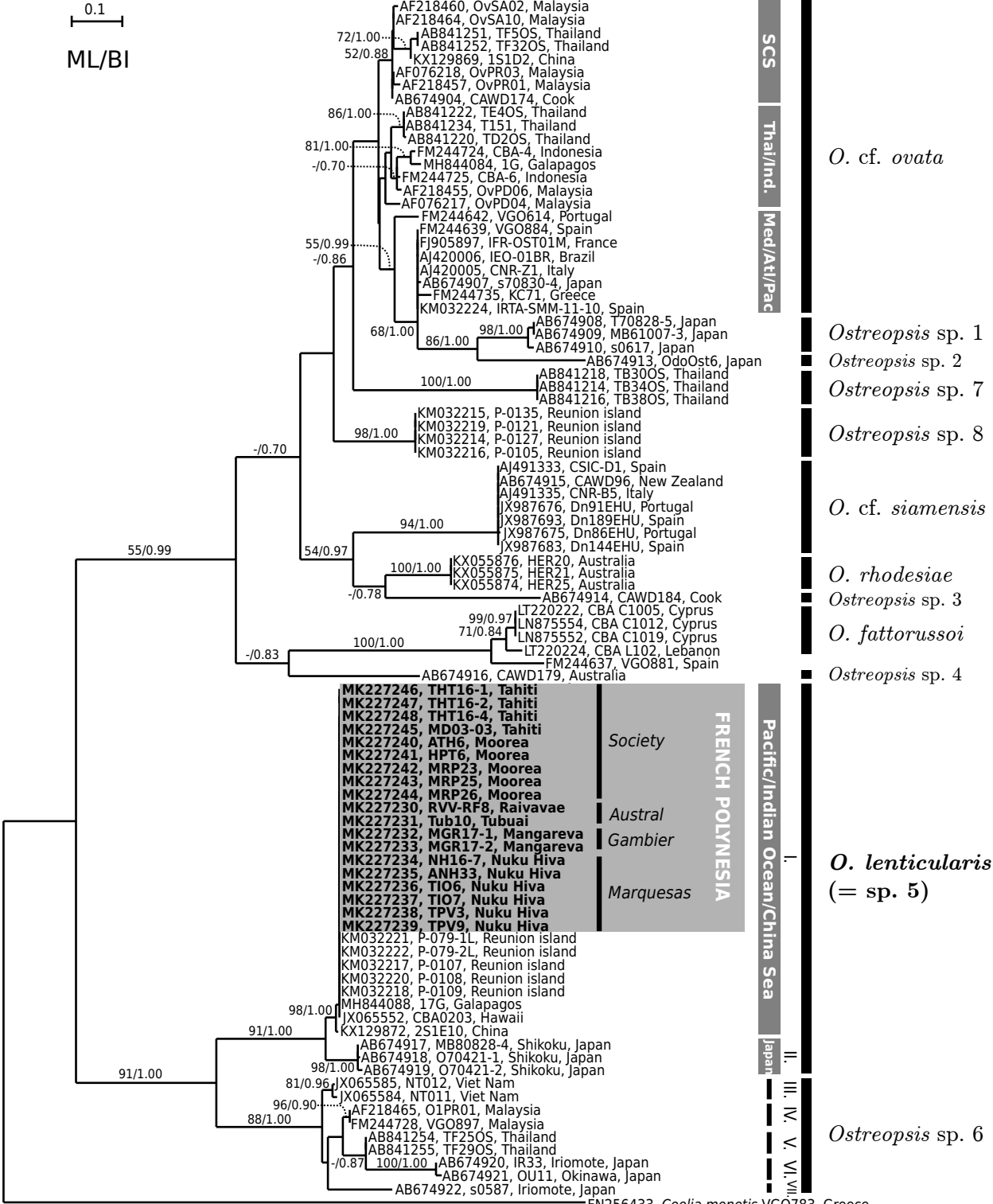
Ostreopsis sp. 6

0.1
ML/BI

SCS
Thal/Ind.
Med/Atl/Pac

FRENCH POLYNESIA
Pacific/Indian Ocean/China Sea

Japan
II.
III.
IV.
V.
VI.
VII.



O. cf. ovata

Ostreopsis sp. 1

Ostreopsis sp. 2

Ostreopsis sp. 7

Ostreopsis sp. 8

O. cf. siamensis

O. rhodesiae

Ostreopsis sp. 3

O. fattorussoi

Ostreopsis sp. 4

O. lenticularis

(= sp. 5)

Ostreopsis sp. 6

Table 1. List of the strains of *Ostreopsis lenticularis* used in the study

Strain	Archipelago	Island, locale	Origin coordinates	isolation date (month-year)	Toxicity analysis (CBA-N2a)	Toxin analysis (LC-MS/MS)	ITS-5.8S rDNA sequences	LSU D8–D10 rDNA sequences
ATH6	Society	Moorea, Atiha	17°35.416S 149°51.013W	May-16	<LOD	–	MK227240	MK227180
HPT6	Society	Moorea, Haapiti	17°35.459S 149°51.580W	May-16	<LOD	–	MK227241	MK227181
MRP23	Society	Moorea, Maharepa	17°28.427S 149°47.000W	May-16	<LOD	–	MK227242	MK227182
MRP25	Society	Moorea, Maharepa	17°28.427S 149°47.000W	May-16	<LOD	–	MK227243	MK227183
MRP26	Society	Moorea, Maharepa	17°28.427S 149°47.000W	May-16	<LOD	–	MK227244	MK227184
MD03-03	Society	Tahiti, Papara	17°47.037S 149°28.088W	Oct.-03	<LOD	<LOD	MK227245 [†]	MK227185
THT16–1	Society	Tahiti, To’ahotu	17°45.247S 149°20.115W	Sept.-16	<LOD	<LOD	MK227246	MK227186
THT16–2	Society	Tahiti, To’ahotu	17°45.247S 149°20.115W	Sept.-16	<LOD	<LOD	MK227247	MK227187
THT16–4	Society	Tahiti, Vairao	17°48.628S 149°18.895W	Sept.-16	<LOD	<LOD	MK227248 [†]	MK227188
VRO17–1	Society	Tahiti, Vairao	17°48.642S 149°18.292W	Aug.-17	–	–	–	MK227189
RVV-RF8	Australes	Raivavae, Rocher de la femme	23°51.914S 147°41.093W	May-08	<LOD	–	MK227230	MK227190
MTR17–1	Australes	Tubuai, Mataura	23°20.375S 149°28.130W	May-17	–	–	–	MK227191
MTR17–2	Australes	Tubuai, Mataura	23°20.375S 149°28.130W	May-17	–	–	–	MK227192
MTR17–3	Australes	Tubuai, Mataura	23°20.375S 149°28.130W	May-17	–	–	–	MK227193
Tub8	Australes	Tubuai, Mataura	23°20.588S 149°28.754W	Oct.-15	–	–	–	MK227194
Tub9	Australes	Tubuai, Mataura	23°20.588S 149°28.754W	Oct.-15	–	–	–	MK227195
Tub10	Australes	Tubuai, Mataura	23°20.588S 149°28.754W	Oct.-15	<LOD	–	MK227231	MK227196
Tub11	Australes	Tubuai, Mataura	23°20.588S 149°28.754W	Oct.-15	–	–	–	MK227197
Tub12	Australes	Tubuai, Mataura	23°20.588S 149°28.754W	Oct.-15	–	–	–	MK227198
Tub14	Australes	Tubuai, Mataura	23°20.588S 149°28.754W	Oct.-15	–	–	–	MK227199
Tub15	Australes	Tubuai, Mataura	23°20.588S 149°28.754W	Oct.-15	–	–	–	MK227200
Tub22	Australes	Tubuai, Mataura	23°20.670S 149°29.241W	Oct.-15	–	–	–	MK227201
Tub23	Australes	Tubuai, Mataura	23°20.670S 149°29.241W	Oct.-15	–	–	–	MK227202
Tub24	Australes	Tubuai, Mataura	23°20.670S 149°29.241W	Oct.-15	–	–	–	MK227203
Tub25	Australes	Tubuai, Mataura	23°20.670S 149°29.241W	Oct.-15	–	–	–	MK227204
Tub26	Australes	Tubuai, Mataura	23°20.670S 149°29.241W	Oct.-15	–	–	–	MK227205

Tub27	Australes	Tubuai, Mataura	23°20.877S 149°29.935W	Oct.-15	–	–	–	MK227206
Tub28	Australes	Tubuai, Mataura	23°20.877S 149°29.935W	Oct.-15	–	–	–	MK227207
Tub29	Australes	Tubuai, Mataura	23°20.877S 149°29.935W	Oct.-15	–	–	–	MK227208
Tub30	Australes	Tubuai, Mataura	23°20.969S 149°30.217W	Oct.-15	–	–	–	MK227209
Tub31	Australes	Tubuai, Mataura	23°20.969S 149°30.217W	Oct.-15	–	–	–	MK227210
Tub32	Australes	Tubuai, Mataura	23°20.969S 149°30.217W	Oct.-15	–	–	–	MK227211
MGR17–1	Gambier	Mangareva, Tenoko	23°04.437S 135°00.581W	Nov.-17	<LOD	–	MK227232	MK227212
MGR17–2	Gambier.	Mangareva, Taku	23°05.240S 134°58.220W	Nov.-17	<LOD	–	MK227233	MK227213
MGR17–3	Gambier	Mangareva, Taku	23°05.240S 134°58.220W	Nov.-17	<LOD	–	–	MK227214
NH16–7	Marquesas	Nuku Hiva, Anaho	08°49.171S 140°03.923W	Nov.-16	<LOD	–	MK227234	MK227215
ANH33	Marquesas	Nuku Hiva, Anaho	08°49.171S 140°03.923W	Nov.-16	<LOD	–	MK227235	MK227216
ANH34	Marquesas	Nuku Hiva, Anaho	08°49.171S 140°03.923W	Nov.-16	<LOD	–	–	MK227217
TIO6	Marquesas	Nuku Hiva, Taiohae	08°56.009S 140°05.581W	Nov.-16	–	–	MK227236	MK227218
TIO7	Marquesas	Nuku Hiva, Taiohae	08°56.009S 140°05.581W	Nov.-16	<LOD	–	MK227237	MK227219
TPV1	Marquesas	Nuku Hiva, Taipivai	08°53.066S 140°02.762W	Nov.-16	–	–	–	MK227220
TPV2	Marquesas	Nuku Hiva, Taipivai	08°53.066S 140°02.762W	Nov.-16	–	–	–	MK227221
TPV3	Marquesas	Nuku Hiva, Taipivai	08°53.066S 140°02.762W	Nov.-16	<LOD	–	MK227238	MK227222
TPV4	Marquesas	Nuku Hiva, Taipivai	08°53.066S 140°02.762W	Nov.-16	–	–	–	MK227223
TPV5	Marquesas	Nuku Hiva, Taipivai	08°53.066S 140°02.762W	Nov.-16	–	–	–	MK227224
TPV6	Marquesas	Nuku Hiva, Taipivai	08°53.066S 140°02.762W	Nov.-16	–	–	–	MK227225
TPV9	Marquesas	Nuku Hiva, Taipivai	08°53.066S 140°02.762W	Nov.-16	–	–	MK227239	MK227226

LOD = limit of detection

†sequence also includes complete SSU and partial LSU rDNA (D1-D3 domains)

Table 2: Distance values (pairwise uncorrected p -distances) based on the LSU D8–D10 rDNA sequences (Clustal W alignment) net-between and within subclades of *O. lenticularis* and *Ostreopsis* sp. 6

Subclade	n	I.	II.	III.	IV.	V.
I. <i>O. lenticularis</i> (subclade French Polynesia / South Japan)	53	0.000				
II. <i>O. lenticularis</i> (subclade North Japan)	10	0.010	0.002			
III. <i>Ostreopsis</i> sp. 6 (subclade IR49, IR33, OU8, OU11)	4	0.051	0.049	0.001		
IV. <i>Ostreopsis</i> sp. 6 (subclade s0595, s0587)	2	0.058	0.058	0.020	0.000	
V. <i>Ostreopsis</i> sp. 6 (subclade TF29OS, TF25OS)	2	0.055	0.055	0.015	0.014	0.000

Pairwise uncorrected p distance values within subclade are shown on the diagonal

Table 3: Distance values (pairwise uncorrected p -distances) based on the ITS–5.8S rDNA sequences (MAFFT alignment) net-between and within subclades of *O. lenticularis* and *Ostreopsis* sp. 6

Subclade	n	I.	II.	III.	IV.	V.	VI.	VII.
<i>O. lenticularis</i>								
I. (subclade Pacific/Indian Ocean/China Sea)	27	0.001						
II. <i>O. lenticularis</i> (subclade Japan)	3	0.068	0.008					
III. <i>Ostreopsis</i> sp. 6 (subclade Vietnam)	2	0.254	0.243	0.012				
IV. <i>Ostreopsis</i> sp. 6 (subclade Malaysia)	2	0.258	0.244	0.057	0.000			
V. <i>Ostreopsis</i> sp. 6 (subclade Thailand)	2	0.267	0.261	0.073	0.048	0.000		
VI. <i>Ostreopsis</i> sp. 6 (subclade IR33, OU11)	2	0.256	0.261	0.135	0.125	0.110	0.010	
VII. <i>Ostreopsis</i> sp. 6 (s0587)	1	0.295	0.282	0.110	0.118	0.118	0.161	–

Pairwise uncorrected p distance values within group are shown on the diagonal